

Effects of the liquid-gas phase transition and cluster formation on the symmetry energy

S. Typel¹, H.H. Wolter², G. Röpke³, and D. Blaschke^{4,5}

¹ GSI Helmholtzzentrum für Schwerionenforschung, Planckstraße 1, 64291 Darmstadt, Germany

² Ludwig-Maximilians-Universität München, Am Coulombwall 1, 85748 Garching, Germany

³ Universität Rostock, Institut für Physik, 18051 Rostock, Germany

⁴ Instytut Fizyki Teoretycznej, Uniwersytet Wrocławski, pl. M. Borna 9, 50-204 Wrocław, Poland

⁵ Bogoliubov Laboratory for Theoretical Physics, JINR Dubna, Joliot-Curie Str. 6, 141980 Dubna, Russia

Received: date / Revised version: date

Abstract. Various definitions of the symmetry energy are introduced for nuclei, dilute nuclear matter below saturation density and stellar matter, which it found in compact stars or core-collapse supernovae. The resulting differences are exemplified by calculations in a theoretical approach based on a generalized relativistic density functional for dense matter. It contains nucleonic clusters as explicit degrees of freedom with medium dependent properties that are derived for light clusters from a quantum statistical approach. With such a model the dissolution of clusters at high densities can be described. The effects of the liquid-gas phase transition in nuclear matter and of cluster formation in stellar matter on the density dependence of the symmetry energy are studied for different temperatures. It is observed that correlations and the formation of inhomogeneous matter at low densities and temperatures causes an increase of the symmetry energy as compared to calculations assuming a uniform uncorrelated spatial distribution of constituent baryons and leptons.

PACS. 21.65.Ef Symmetry energy – 21.60.Jz Nuclear Density Functional Theory and extensions – 05.30.-d Quantum statistical mechanics – 05.70.Fh Phase transitions: general studies

1 Introduction

The isospin degree of freedom [1,2] is a particular feature of systems that contain strongly interacting particles. The (a)symmetry energy characterizes how much the energy of the system changes when the isospin resp. the asymmetry is varied keeping other quantities and quantum numbers constant. Historically, the symmetry energy appeared first in the description of binding energies of finite nuclei [3,4]. Later, the concept was generalized to nuclear matter. It has proven to be enormously valuable in nuclear physics. The dependence of the symmetry energy on density and temperature is of particular interest because there are tight connections to observable properties of atomic nuclei, neutron matter, heavy-ion collisions and compact stars. Many studies are devoted to understand and quantify these relations, see, e.g., the recent works [5,6,7,8,9,10,11,12,13,14,15,16,17,18,19,20,21], references cited therein, and the contributions to this volume of the European Physical Journal A.

A meaningful comparison of the symmetry energy in experiment and theory relies on a precise definition of this quantity. Since different methods are used to extract the symmetry energy from measurements and calculations, the relation between the obtained values has to be under-

stood. The deduced symmetry energies may depend on the particular system that is investigated and thermodynamic conditions have to be taken into account. These differences due to different definitions are more pronounced at densities below the nuclear saturation density. Thus, we will concentrate on this region in the present work.

Dense matter will be treated only in the thermodynamic limit of infinite volume and particle number. Finite size systems with a limited number of particles, as they appear in laboratory experiments, may differ in their properties from the infinite systems. Their theoretical description requires to choose the appropriate thermodynamic ensemble and the derived symmetry energies can depend on this choice.

In the laboratory, the equation of state can be studied in heavy-ion collisions. In such processes the matter may even be out of thermodynamic equilibrium. The derivation of densities and temperatures of equivalent systems in thermodynamic equilibrium is rather involved and may depend on particular model assumptions. However, this is not the topic of our present work. A recent discussion of results from laboratory experiments with heavy-ion collisions is given by Hagel et. al. [22] in this volume. Recent experimental approaches to extract the nuclear symmetry energy from light fragment yields are based on the isocal-

ing method [23,24,25]. There the symmetry free energy is obtained by studying collisions of nuclei with different neutron numbers as a function of the asymmetry.

Dense matter is often treated as a spatially homogeneous system of strongly interacting particles considering only baryons and mesons and the symmetry energy is calculated under this condition in theoretical models. However, due to the interaction between the constituents, correlations are an important feature that can lead to the formation of clusters [26,27,28,29,30,31,32,33]. Light clusters, like deuterons or alpha particles, but also heavy nuclei, which are embedded in the matter, will appear. In this case, clusters move freely and the matter can still be considered homogeneous on length scales sufficiently larger than the cluster sizes. At larger densities, just below nuclear saturation density, “pasta phases” can arise, which, however, are not considered here. On the other hand, phase transitions with macroscopic regions of low and high densities can occur, see Ref. [34,35,36,37]. Both these phenomena will be considered in the present work. They can have significant effects on the density dependence of the symmetry energy.

In conventional model calculations the symmetry energy vanishes linearly with decreasing density. Experimental results suggest considerably higher values in the low-density limit [23,24] as compared to such a linear density dependence. The modification of this behavior is described in a quantum statistical approach as a result of cluster formation, which is, however, strongly temperature dependent. With increasing density a good agreement with other estimates is obtained [38].

It is important to distinguish between finite nuclei, nuclear matter and stellar matter. The last two are infinite systems, where in nuclear matter the Coulomb interaction is turned off, while in stellar matter it is compensated by a lepton component requiring global charge neutrality. All these systems have substantially different phase structures and chemical compositions.

The aim of the present work is the following. After introducing the original definition of the symmetry energy in nuclei, we consider those used in theoretical models for matter of finite density. These definitions are applied to calculations in a theoretical model, which describes nuclear matter and stellar matter in a consistent approach, and the resulting differences of different definitions are discussed. The effects of cluster correlations and of the liquid-gas phase transition are explored. Here the question of separating strong and electromagnetic contributions to the energy will be seen to be important in order to allow for meaningful comparisons and to be consistent with the separation of energy contributions for finite nuclei. This review is a continuation of our previous works on cluster correlations in matter [27,31,32] with particular emphasis on the consequences for the symmetry energy in different systems.

The content of this work is as follows: First, in section 2, several quantities to characterize the variation of the energy of a system as a function of the independent variables are introduced. In particular, different theoretic-

cal definitions of the symmetry energy in nuclei and infinite matter without cluster formation will be considered. In section 3 a model for matter of finite density is presented that is based on a generalized relativistic density functional (gRDF) approach with nucleons, clusters and electrons (for stellar matter) as constituent particles, where the medium properties of the clusters are calculated from a quantumstatistical model. The density functional approach allows to study and to compare quantitatively the different definitions of the symmetry energy in the considered systems under various thermodynamic conditions. The conclusions are summarized in section 4. Details about the liquid-gas phase transition construction, the medium dependent mass shifts of the clusters and the effective degeneracy factors of heavy nuclei can be found in the appendices A, B, and C, respectively. Throughout this work we use the traditional nuclear system of units where $\hbar = c = k_B = 1$.

2 Definitions of the symmetry energy

The definition of the symmetry energy depends on the type of system and the thermodynamic conditions. In the following, various ways to introduce the symmetry energy and their relations will be discussed.

2.1 Nuclei

For a nucleus with N neutrons and Z protons, the asymmetry δ is given by

$$\delta = \frac{N - Z}{N + Z}, \quad (1)$$

which corresponds to the third component of the isospin I_z . The binding energies $B(N, Z)$ of isobaric nuclei, i.e. nuclei with equal mass number $A = N + Z$, show a characteristic variation with the asymmetry δ that is almost symmetric with respect to an exchange of neutrons and protons for light nuclei. The contribution of the electromagnetic interaction to the energy leads to a violation of this symmetry, which is more severe for heavier nuclei with larger charge numbers. The isospin dependence is reflected in the semi-empirical or Bethe-Weizsäcker mass formula [3, 4, 39] for nuclei. In this average description, the binding energy of a nucleus is given by

$$B(N, Z) = a_V A - a_S A^{2/3} - \left(a_V^{(\text{sym})} A + a_S^{(\text{sym})} A^{2/3} \right) \delta^2 - a_C \frac{Z(Z-1)}{A^{1/3}} + \dots \quad (2)$$

with volume, surface, volume symmetry, surface symmetry and Coulomb contributions that show a particular dependence on the mass number A and asymmetry δ . The introduction of a surface symmetry term improves the description of the binding energies and allows to better separate the mass number dependence of the volume symmetry energy of infinite matter. Various forms for the total

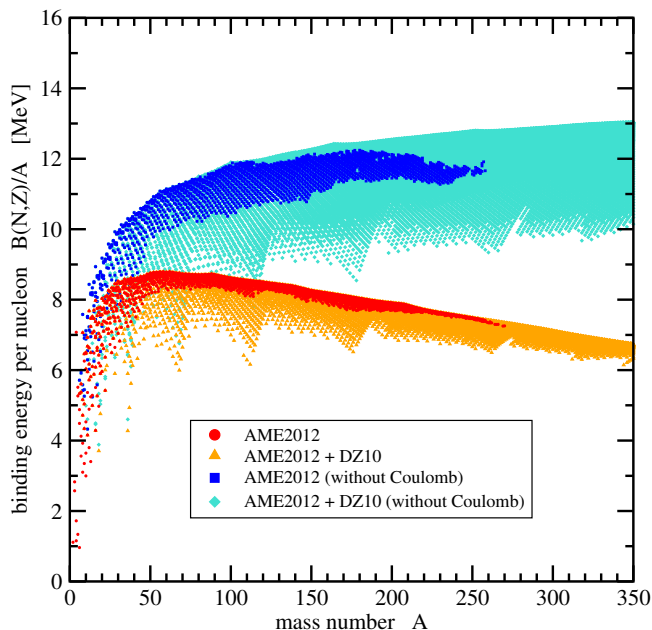


Fig. 1. Binding energy per nucleon $B(N, Z)/A$ as a function of the mass number A for all nuclei of the AME2012 atomic mass evaluation [41] and the DZ10 mass model [42] with and without the Coulomb contribution $E_{\text{Coul}}(N, Z)$. See text for details.

symmetry energy are introduced in the literature, see e.g. Ref. [40], which takes thermodynamic considerations into account. Pairing and other features such as shell effects are not considered here. The parameters a_V , a_S , $a_V^{(\text{sym})}$, $a_S^{(\text{sym})}$, a_C are found by fitting nuclear masses

$$m_{N,Z} = Nm_n + Zm_p - B(N, Z) \quad (3)$$

across the whole chart of nuclei. Here m_n and m_p are the neutron and proton rest masses, respectively. Typical values of the coefficients are $a_V = 15.73$ MeV, $a_S = 17.77$ MeV, $a_V^{(\text{sym})} = 26.46$ MeV, $a_S^{(\text{sym})} = -17.70$ MeV, and $a_C = 0.709$ MeV [39].

The binding energy per nucleon $B(N, Z)$ for four sets of nuclei is shown in figure 1 as a function of the mass number A . The first set (red circles) includes all nuclei with experimentally known binding energies of the AME2012 atomic mass evaluation [41]. The second set (orange triangles) is an extension of the first set. It is obtained by adding all nuclei with binding energy predictions of the DZ10 mass formula [42], which gives a rather good fit of the known masses. All nuclei with $A \leq 350$ and positive neutron and proton separation energies are included. The usual pattern is observed with signs of shell closures, a maximum in the iron region and a smooth reduction of the binding energy per nucleon with increasing mass number A beyond the maximum. The third set (dark blue squares) covers the same nuclei as set 1 but the Coulomb energy

$$E_{\text{Coul}} = a_C \frac{Z(Z-1)}{A^{1/3}} \quad (4)$$

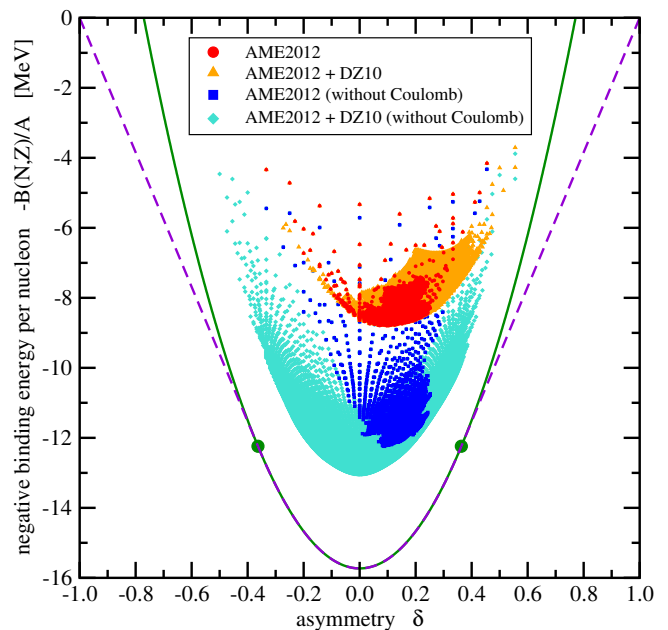


Fig. 2. Negative binding energy per nucleon $-B(N, Z)/A$ as a function of the asymmetry δ for all nuclei with $A \leq 350$ of the atomic mass evaluation AME2012 and the DZ10 mass formula [42] with and without the Coulomb contribution $E_{\text{Coul}}(N, Z)$. The full green line is the infinite- A limit (5) of the Bethe-Weizsäcker formula and the green circles denote the neutron and proton drip points on this line. The dashed violet line extends the full green curve in the range $|\delta| \leq \delta_{\text{drip}}$ by interpolating between the drip points and the case $|\delta| = 1$ with unbound neutrons and protons only. See text for details.

with $a_C = 3e^2/(5r_0)$, is removed from the binding energies of nuclei. Using the standard value $r_0 = 1.25$ fm for the radius parameter, we have $a_C = 0.6912$ MeV, which is slightly different from the values derived in actual fits to binding energies. The same transformation is applied to the second set to obtain the fourth set (light blue diamonds). The differences to the first two sets are obvious. There is a continuous increase of the binding energy per nucleon with A . In sets 2 and 4, the variation of the $B(N, Z)/A$ for constant A reflects the isospin dependence for isobaric nuclei. A larger number of nuclei appears in the fourth set since without the Coulomb contribution to the binding energy the neutron and proton driplines are shifted to much more exotic nuclei, in particular for proton-rich nuclei.

In figure 2 the same sets of nuclei as in figure 1 are considered but now the negative binding energy per nucleon is depicted as a function of the asymmetry parameter δ . The sets 1 and 2 that include the Coulomb contribution to the binding energy show a minimum at $\delta \neq 0$ since the isospin symmetry is clearly broken due to the Coulomb interaction. When the Coulomb energy E_{Coul} is removed from $B(N, Z)$, the distribution becomes more or less symmetric in δ with a minimum at $\delta = 0$. Constructing the lower bound of $-B(N, Z)$ for the nuclei of set 4, a piecewise linear function is obtained that can be well approxi-

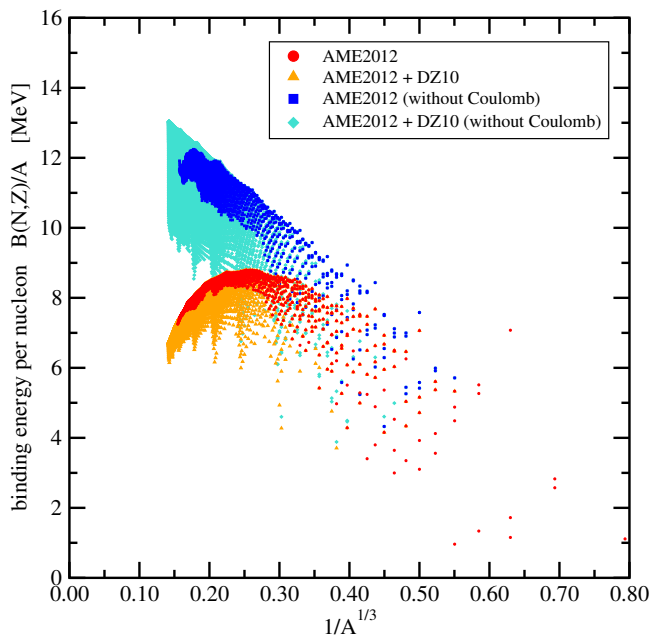


Fig. 3. Binding energy per nucleon $B(N, Z)/A$ as a function of the inverse cubic root of the mass number, $1/A^{1/3}$, for all nuclei with $A \leq 350$ of the AME2012 atomic mass evaluation [41] and the DZ10 mass model [42] with and without the Coulomb contribution $E_{\text{Coul}}(N, Z)$. For the latter one can extrapolate to the infinite system and obtains the volume coefficient a_V of the symmetric matter binding energy functional. See text for details.

ated by a quadratic function of δ close to the minimum. Since the selection of nuclei in set 4 is limited to those with mass number $A \leq 350$ the minimum curve does not represent the infinite nuclear matter result. The curve will move downwards when more massive nuclei are included.

In the limit $A \rightarrow \infty$ and neglecting the Coulomb contribution to $B(N, Z)$, only the two bulk contributions to the binding energy per nucleon

$$B(N, Z)/A \rightarrow B_\infty(\delta) = a_V - a_V^{(\text{sym})} \delta^2, \quad (5)$$

remain. The corresponding curve (with $a_V = 15.73$ MeV and $a_V^{(\text{sym})} = 26.46$ MeV) is shown in figure 2 by the full green line. The minimum is given by $-a_V$ where the coefficient a_V is identified with the bulk binding energy B_{sat} of cold saturated infinite nuclear matter. It can be obtained also by extrapolating the dependence of $B(N, Z)/A$ on the inverse size of the system to $\lim_{A \rightarrow \infty} 1/A^{1/3} = 0$ for the case without the Coulomb contribution, see figure 3.

Similarly, $a_V^{(\text{sym})}$ is the bulk nuclear symmetry energy at saturation and can be regarded as the symmetry energy of nuclear matter denoted below as J . Note, that the parameter $a_V^{(\text{sym})}$ is found from fits to experimental data to all nuclei, which follow only approximately equation (2). It is neither obtained from a second derivative nor from a finite difference of energies as in the case of infinite matter (see below).

For asymmetries $\delta = \pm 1$, the quadratic form (5) predicts negative binding energies per nucleon since $a_V < a_V^{(\text{sym})}$, i.e. unbound systems. In fact, the curve should terminate at finite values of δ when the neutron and proton driplines are reached. In the limit $A \rightarrow \infty$ this corresponds to the conditions

$$\left. \frac{d}{dN} \frac{B(N, Z)}{A} \right|_{\delta=\delta_{\text{drip}}} = 0 \quad (6)$$

and

$$\left. \frac{d}{dZ} \frac{B(N, Z)}{A} \right|_{\delta=-\delta_{\text{drip}}} = 0 \quad (7)$$

that are obtained at the drip asymmetry δ_{drip} . The value is found to be

$$\delta_{\text{drip}} = 1 - \sqrt{1 - \frac{a_V}{a_V^{(\text{sym})}}} \quad (8)$$

with $\delta_{\text{drip}} = 0.3632$ for the above given parameters. These dripline points are denoted in figure 2 by the green circles.

The most extreme values $\delta = \pm 1$ correspond to pure neutrons or protons with zero binding energy. Connecting these points with the dripline points on the full green line, the dashed violet line is obtained, which is a quadratic function for $|\delta| \leq \delta_{\text{drip}}$ and a linear function for $|\delta| \geq \delta_{\text{drip}}$. This curve can be interpreted as the binding energy per nucleon of infinite nuclear matter in the zero-density limit at zero temperature. Since the energy per nucleon for $\delta = 0$ is non-vanishing, a finite symmetry energy can be anticipated in this case, see subsection 3.2. Following thermodynamical considerations, it is a convex function of δ . The transition asymmetry δ_t where the quadratic behavior changes to a linear one is easily found from the condition

$$-\left. \frac{dB_\infty}{d\delta} \right|_{\delta=\delta_t} = \frac{B_\infty(\delta_t)}{1 - \delta_t} \quad (9)$$

to be identical with the drip asymmetry (8).

Since a particular nucleus has a fixed number of neutrons and protons, it is not reasonable to define the symmetry energy for a specific nucleus itself. It is a property that characterizes the set of all nuclei. However, if nuclei are studied in a hot and dense environment, their energies are different as compared to those in vacuum and, correspondingly, the coefficients in a generalized Bethe-Weizsäcker formula can depend on the medium properties such as temperature and density if such a description is applied.

2.2 Infinite matter at finite density

The concept of symmetry energy can also be applied to infinite matter at zero and finite temperature. However, there is a fundamental difference between nuclear matter and stellar matter with considerably distinct phase diagrams. The former is a theoretical model for a system of strongly interacting particles neglecting the electromagnetic interaction because it gives a diverging contribution in infinite systems. In contrast, for stellar matter

that occurs in compact stars or core-collapse supernovae, both the strong and electromagnetic interactions are taken into account. The condition of global charge neutrality requires to include charged leptons, in particular electrons. There are (at least) two independent conserved charges in infinite matter: the total baryon number and the total charge number. More exist, if strangeness and other lepton species are considered. Correspondingly, one can define a total baryon number density n_B and a charge number density n_Q . For a system with N_n neutrons and N_p protons in a volume V , these densities are given by $n_B = (N_n + N_p)/V$ and $n_Q = N_p/V = (1 - \delta)n_B/2$. Then, the energy per particle E can be expressed as a function of n_B and n_Q or, more conveniently, n_B and the asymmetry δ . The functional dependence of the energy per particle on n_B and δ is also appropriate for stellar matter since the number density of charged leptons n_L (electrons and, at high densities, muons) is determined via the charge neutrality condition.

2.2.1 Nuclear matter

At low temperatures, nuclear matter exhibits the phenomenon of saturation as a result of the competition of long-range attraction and short-range repulsion between the nucleons. Due to the isospin symmetry of the strong interaction, the system assumes its lowest energy for asymmetry $\delta = 0$ and zero temperature at the saturation baryon density n_{sat} if the neutron-proton mass difference is neglected. The energy per particle (without the rest mass contribution) in cold nuclear matter, i.e. at zero temperature, can be expressed as

$$E(n_B, \delta) = E_0(n_B) + E_{\text{sym}}(n_B) \delta^2 + \mathcal{O}(\delta^4) \quad (10)$$

with the energy per particle of symmetric nuclear matter $E_0(n_B) = E(n_B, 0)$ and the density dependent symmetry energy

$$E_{\text{sym}}(n_B) = \frac{1}{2} \frac{\partial^2}{\partial \delta^2} E(n_B, \delta) \Big|_{\delta=0}, \quad (11)$$

sometimes denoted by $S(n_B)$. The quadratic behavior for the dependence on δ in eq. (10) must be valid in the sense of an expansion in δ around zero due to the isospin symmetry of nuclear forces. It is often also well justified in homogeneous matter for larger ranges of δ . Deviations from the quadratic behavior are generally small except for baryon densities much different from the saturation density $n_{\text{sat}} \approx 0.16$ fm⁻³.

It has been customary to expand the energy of symmetric nuclear matter close to the saturation point as

$$E_0(n_B) = -B_{\text{sat}} + \frac{1}{2} K x^2 + \frac{1}{6} K' x^3 + \dots \quad (12)$$

for small $x = (n_B/n_{\text{sat}} - 1)/3$. There is no term linear in x due to the minimum condition at $x = 0$. The coefficient $B_{\text{sat}} = E_0(n_{\text{sat}})$ is identified with a_V in the Bethe-Weizsäcker formula. The coefficients

$$K = 9n_B^2 \frac{d^2}{dn_B^2} E_0(n_B) \Big|_{n_B=n_{\text{sat}}} \quad (13)$$

and

$$K' = 27n_B^3 \frac{d^3}{dn_B^3} E_0(n_B) \Big|_{n_B=n_{\text{sat}}} \quad (14)$$

are the (in)compressibility of bulk nuclear matter and the skewness coefficient, respectively. In a similar way the symmetry energy admits an expansion

$$E_{\text{sym}}(n_B) = J + Lx + \frac{1}{2} K_{\text{sym}} x^2 + \dots \quad (15)$$

with the symmetry energy at saturation

$$J = E_{\text{sym}}(n_{\text{sat}}) \equiv a_V^{(\text{sym})}, \quad (16)$$

the slope parameter

$$L = 3n_{\text{sat}} \frac{d}{dn_B} E_{\text{sym}}(n_B) \Big|_{n_B=n_{\text{sat}}} \quad (17)$$

and the symmetry curvature or symmetry incompressibility

$$K_{\text{sym}} = 9n_B^2 \frac{d^2}{dn_B^2} E_{\text{sym}}(n_B) \Big|_{n_B=n_{\text{sat}}}. \quad (18)$$

It has been a major aim of recent efforts in nuclear physics to determine values for these characteristic parameters of cold nuclear matter from various experiments, see, e.g., the contribution of X. Viñas et al. in this volume [43].

Instead of the quantity L , the symmetry pressure $p_0 = Ln_{\text{sat}}/3$ is introduced in some works. In a different representation of the density dependence of the symmetry energy it is sometimes separated into a kinetic and a potential term as

$$E_{\text{sym}}(n_B) = C_{\text{kin}} \left(\frac{n_B}{n_{\text{sat}}} \right)^{2/3} + C_{\text{pot}} \left(\frac{n_B}{n_{\text{sat}}} \right)^\gamma \quad (19)$$

with ($m_{\text{nuc}} \approx m_n \approx m_p \approx 939$ MeV)

$$C_{\text{kin}} = \frac{1}{6m_{\text{nuc}}} \left(\frac{3\pi^2}{2} n_{\text{sat}} \right)^{2/3}. \quad (20)$$

The coefficients C_{pot} and γ parametrize the density dependence of the symmetry energy in the region of saturation density. At saturation we have

$$C_{\text{pot}} = J - C_{\text{kin}}. \quad (21)$$

The kinetic term originates from an expansion of the energy of a free Fermi gas of neutrons and protons

$$\begin{aligned} E_{\text{kin}}(n_B, \delta) & \quad (22) \\ &= \frac{3}{10m_{\text{nuc}}} (3\pi^2 n_B)^{2/3} \\ & \times \left[\left(\frac{1+\delta}{2} \right)^{5/3} + \left(\frac{1-\delta}{2} \right)^{5/3} \right] \\ &= \frac{3}{10m_{\text{nuc}}} \left(\frac{3\pi^2}{2} n_B \right)^{2/3} \left[1 + \frac{5}{9} \delta^2 + \mathcal{O}(\delta^4) \right]. \end{aligned}$$

However, sometimes the effect of correlations has been introduced into the kinetic energy term, see the contribution [44] in this volume and references therein, e.g. by introducing an effective mass. The parameter γ in equation (19) determines the slope

$$L = 2C_{\text{kin}} + 3\gamma C_{\text{pot}} = (2 - 3\gamma)C_{\text{kin}} + 3\gamma J \quad (23)$$

at the saturation density n_{sat} . However, the slope L is not independent of the assumptions on C_{kin} and J . For $C_{\text{kin}} = 12$ MeV, $J = 32$ MeV, and $\gamma = 1$ the value $L = 84$ MeV is obtained for the slope parameter.

Nuclear matter can also be considered at finite temperatures T . From a thermodynamic point of view, the appropriate quantity to be studied is the free energy density $f(T, n_B, n_Q)$ or the free energy per particle $F(T, n_B, \delta) = f(T, n_B, n_Q)/n_B$ because temperature and densities are the natural variables in this case. The free energy per particle can be expanded for small asymmetries as

$$F(T, n_B, \delta) = F_0(T, n_B) + F_{\text{sym}}(T, n_B) \delta^2 + \mathcal{O}(\delta^4) \quad (24)$$

like in equation (10) with the free energy per particle of symmetric nuclear matter $F_0(T, n_B) = F(T, n_B, 0)$ and the symmetry free energy

$$F_{\text{sym}}(T, n_B) = \frac{1}{2} \left. \frac{\partial^2}{\partial \delta^2} F(T, n_B, \delta) \right|_{\delta=0}. \quad (25)$$

Both quantities are functions of temperature and baryon density. For zero temperature the usual symmetry energy $E_{\text{sym}}(n_B) = F_{\text{sym}}(0, n_B)$ is recovered.

Instead of the free energy per particle (24), one can consider the internal energy per particle U . From the standard relations of thermodynamics between free and internal energies with the entropy per particle S we obtain the symmetry internal energy per particle

$$U_{\text{sym}}(T, n_B) = F_{\text{sym}}(T, n_B) + TS_{\text{sym}}(T, n_B) \quad (26)$$

with the symmetry entropy per particle

$$\begin{aligned} S_{\text{sym}}(T, n_B) &= -\frac{1}{2} \left. \frac{\partial^2}{\partial \delta^2} \frac{\partial}{\partial T} F(T, n_B, \delta) \right|_{\delta=0} \\ &= -\frac{\partial}{\partial T} F_{\text{sym}}(T, n_B). \end{aligned} \quad (27)$$

Hence, there is a difference between symmetry free energies and symmetry internal energies, which can be substantial for large temperatures. However, another definition of the symmetry internal energy can be introduced because T is not the natural variable of the thermodynamic potential U . In fact, the natural variables are the entropy per particle S and the baryon number and charge number densities. Then, the expansion for small symmetries reads

$$U(S, n_B, \delta) = U_0(S, n_B) + U_{\text{sym}}(S, n_B) \delta^2 + \mathcal{O}(\delta^4) \quad (28)$$

with the symmetry internal energy

$$U_{\text{sym}}(S, n_B) = \frac{1}{2} \left. \frac{\partial^2}{\partial \delta^2} U(S, n_B, \delta) \right|_{\delta=0}. \quad (29)$$

Employing standard thermodynamic identities, the relations

$$\left. \frac{\partial}{\partial \delta} F(T, n_B, \delta) \right|_{T, n_B} = \left. \frac{\partial}{\partial \delta} U(S, n_B, \delta) \right|_{S, n_B} \quad (30)$$

and

$$\begin{aligned} F_{\text{sym}}(T, n_B) &= U_{\text{sym}}(S, n_B) \\ &+ \frac{1}{2} \left. \frac{\partial T}{\partial \delta} \right|_{S, n_B, \delta=0} \left. \frac{\partial S}{\partial \delta} \right|_{T, n_B, \delta=0} \end{aligned} \quad (31)$$

are found. Obviously, the isospin dependence of the energy in systems with equal entropy per particle and baryon density has to be distinguished from that of systems with equal temperature and baryon density. In the following, only symmetry energies in systems of constant temperature will be considered.

The definitions (11), (25), and (29) using second derivatives are motivated by the expansion of the energy per particle in nuclear matter near saturation density in a power series in δ . Assuming a quadratic dependence on the asymmetry δ for the whole range of δ these definitions can be replaced by finite difference formulas, e.g.

$$\begin{aligned} E_{\text{sym}}(n_B) & \\ &= \frac{1}{2} [E(n_B, +1) - 2E(n_B, 0) + E(n_B, -1)] \end{aligned} \quad (32)$$

and similar for the free energy per particle F and the internal energy per particle U with identical results for the two definitions. In this case, the energy of symmetric matter ($\delta = 0$) is compared to pure neutron ($\delta = 1$) and pure proton ($\delta = -1$) matter. In many cases, however, there is a difference of these definitions using second derivatives or finite differences due to deviations from the δ^2 dependence of the energies for finite values of δ as will be shown below and was discussed already in Ref. [27]. The derivative is not always well defined and can diverge if, e.g., light clusters at very low temperatures are considered in the model, see Ref. [27]. The finite-difference formula (32) is always applicable. We will show that it represents the effect of the isospin dependence adequately.

For low temperatures T , the pressure

$$p(T, n_B, \delta) = n_B^2 \left. \frac{\partial F}{\partial n_B} \right|_{T, \delta} \quad (33)$$

can become negative for densities n_B lower than the saturation density n_{sat} . This behavior indicates that nuclear matter becomes unstable against density fluctuations in this region. As a consequence, the system will no longer remain spatially homogeneous. Finite-size clusters will form separating regions of high and low densities. Since an increase of the cluster size will lead to a larger binding energy per particle in general, cf. the Bethe-Weizsäcker formula (2) without the Coulomb contribution, the whole system will separate into two macroscopic phases in the infinite volume limit and the well-known liquid-gas phase transition will emerge. The correct state in thermodynamic equilibrium can be found, e.g., by minimizing the

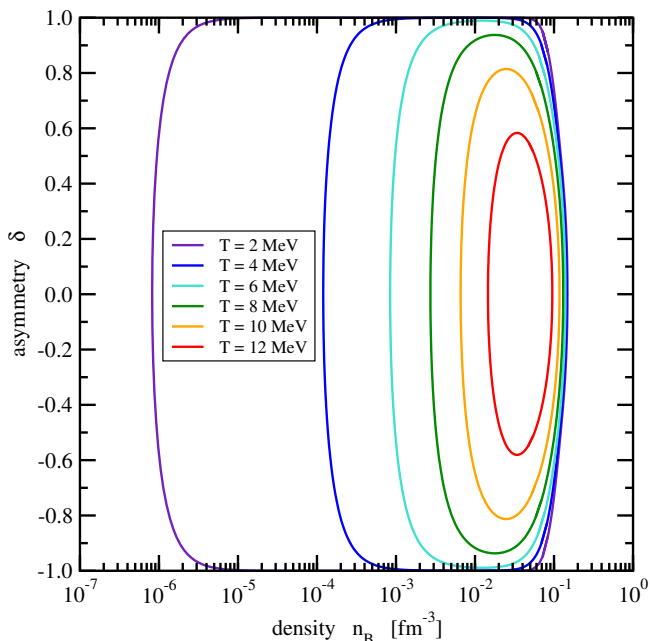


Fig. 4. Binodals of nuclear matter in the gRDF model for various temperatures T in the asymmetry-density plane. Cluster formation is not taken into account.

free energy density $f(T, n_B, n_Q)$ globally. Since there are two conserved charges, corresponding to the independent particle densities n_B and n_Q , in the system, a “noncongruent” phase transition is the result [34, 35, 36, 37]. The thermodynamic quantities in the region of coexisting phases can be constructed using the well-known Gibbs conditions, i.e. the equality of all intensive thermodynamic variables in all phases. See appendix A for details.

The boundaries of the phase coexistence region or “binodals” are depicted for various temperatures in figure 4 for the gRDF model of section 3 without clusters. With decreasing temperature, the enclosed coexistence region grows and covers larger sections of the asymmetry-density plane; with larger asymmetry the region of coexistence shrinks. Above the critical temperature $T_{\text{crit}} = 13.724$ MeV of the gRDF model for nuclear matter, there is no separation of phases. The critical baryon density for the gRDF model without clusters is $n_B^{(\text{crit})} = 0.04515 \text{ fm}^{-3}$. Due to a finite symmetry energy, the isospin asymmetries in the two coexisting phases will be different for a system with asymmetry $\delta \neq 0$. The high-density phase (liquid) is found to be more isospin symmetric and the low-density phase (gas) more isospin asymmetric. This behavior has sometimes been called isospin distillation or fractionation, see, e.g., Ref. [45]. The existence of the liquid-gas phase transition in nuclear matter affects the density dependence of the symmetry energy. This will be studied in section 3.

2.2.2 Stellar matter

Stellar matter in compact stars or core-collapse supernovae represents a system containing strongly and electro-

magnetically interacting particles. It is considerably different from nuclear matter in respect to thermodynamic properties. The charge of particles cannot be neglected and the condition of total charge neutrality requires to include electrons as constituent particles. They form a homogeneous distribution of degenerate fermions at sufficiently high densities. Since the electronic background is not completely incompressible, the interaction between electrons and charged baryonic particles can induce electron-cluster correlations with a local increase of the electron density near clusters. This effect can be treated approximately in calculations by employing the Wigner-Seitz approximation.

Correlations due to the strong and electromagnetic interactions affect the phase structure of the system in a different way as compared to nuclear matter. The competition between the attractive nuclear interaction and the repulsive Coulomb interaction favors the formation of finite-size structures [35], e.g. clusters. The Coulomb contribution to the cluster energy is screened by the electron background leading to an increased binding. Considering the full table of nuclei, this causes a shift of the position of the most-bound nucleus to larger mass numbers. Furthermore, the properties of nuclei in the medium are modified as compared to their vacuum values as a consequence of the Pauli exclusion principle and the impact of the nuclear interaction. Note that the results for nuclear matter in the previous subsection were obtained without cluster formation.

The definitions of the symmetry energy that were introduced for infinite nuclear matter can be transferred directly to the stellar matter case. However, since the contribution of electrons and the electromagnetic interaction are included, the energy of the matter does not show a simple isospin symmetry any more. At very low temperatures and not too high densities, stellar matter undergoes a phase transition to a Wigner crystal indicating the importance of long-range Coulomb correlations. At higher densities, so-called “pasta” phases appear. Due to all these features, the extraction of a symmetry energy in stellar matter will yield results that can be different to nuclear matter. Appropriate modifications have to be applied in order to give comparable quantities, in particular a correction for the Coulomb contribution.

In core-collapse supernovae, the properties of stellar matter are probed in a large range of asymmetries δ . In cold compact stars, however, stellar matter will be in β equilibrium and the asymmetry is fully determined due to the simultaneously required condition of charge neutrality. Assuming an ideal mixture of (interacting) nucleons and relativistic electrons, the total energy density at zero temperature is given by

$$\begin{aligned} \varepsilon_{\text{tot}}(n_n, n_p, n_e) & \quad (34) \\ & = m_n n_n + m_p n_p + E(n_B, \delta) n_B + \frac{3}{4} E_e n_e + \frac{1}{4} m_e n_e^{(s)} \end{aligned}$$

with

$$E_e = \sqrt{k_e^2 + m_e^2}, \quad (35)$$

the electron Fermi momentum

$$k_e = (3\pi^2 n_e)^{1/3}, \quad (36)$$

which depends on the electron density n_e , and the scalar electron density

$$n_e^{(s)} = \frac{m_e}{2\pi^2} \left[k_e E_e - m_e^2 \ln \frac{k_e + E_e}{m_e} \right]. \quad (37)$$

The condition of β equilibrium can be expressed as

$$\mu_n = \mu_p + \mu_e \quad (38)$$

with the chemical potentials

$$\mu_i = \left. \frac{\partial \varepsilon_{\text{tot}}}{\partial n_i} \right|_{n_j \neq i} \quad (39)$$

of the particles $i = n, p, e$. Considering charge neutrality, i.e. $n_e = n_p = (1 - \delta)n_B/2$ and assuming in eq. (10) a purely quadratic dependence of the nuclear matter energy $E(n_B, \delta)$ on δ (without the electronic contribution), the asymmetry $\delta_\beta(n_B)$ at β equilibrium is determined by the condition (c.f. Ref. [46])

$$4\delta_\beta E_{\text{sym}}(n_B) + m_n - m_p = \mu_e(n_B, \delta_\beta) \quad (40)$$

with

$$\mu_e(n_B, \delta_\beta) = E_e \quad (41)$$

and thus determined by the density dependence of the symmetry energy.

3 Generalized relativistic density functional for dense matter

In order to illustrate the effects of the liquid-gas phase transition in nuclear matter without clustering and of cluster formation in stellar matter on the symmetry energy, a theoretical model is required that is able to describe these features. We adopt, extend and modify the approach of Refs. [27,31] that is based on a relativistic mean-field model for nuclear matter and nuclei with density dependent meson-nucleon couplings. Besides nucleons, light and heavy clusters are included as degrees of freedom with medium dependent properties.

3.1 Thermodynamic quantities

Using a grand canonical description, all relevant thermodynamic quantities can be derived from the grand canonical potential density $\omega_{gc}(T, \mu_i)$ that is a function of the temperature T and chemical potentials μ_i of all constituents. In the case of nuclear matter, only neutrons ($i = n$) and protons ($i = p$) are considered. For stellar matter, also nuclei ($i = (N, Z)$) and electrons ($i = e$) are included as degrees of freedom. In order to reproduce the model independent virial equation of state at low baryon densities,

see. e.g. [47,48,49], also two-nucleon continuum correlations ($i = (nn)_{T=1}, (np)_{T=1}, (np)_{T=0}, (pp)_{T=1}$) in the appropriate isospin channels are introduced and represented by effective medium dependent cluster resonance states. The effects of the strong interaction are modeled by the exchange of effective mesons ($m = \sigma, \omega, \rho$) that couple minimally to the free nucleons and nucleons in clusters.

A baryon number B_i , a charge number Q_i and an (electronic) lepton number L_i are associated to each particle i . For clusters, we have $B_i = N_i + Z_i = A_i$, $Q_i = Z_i$, and $L_i = 0$ whereas for electrons $B_e = 0$, $Q_e = -1$, and $L_e = 1$.

Every particle with rest mass m_i in the vacuum is considered as a quasiparticle with energy

$$E_i(k) = \sqrt{k^2 + (m_i - S_i)^2} + V_i \quad (42)$$

that depends on the particle momentum k , the scalar potential S_i , and the vector potential V_i . These potentials contain effects of the strong and electromagnetic interaction and of the medium modification of particle properties.

Experimental rest masses are used for neutrons, protons and electrons. The rest masses of clusters are given by

$$m_i = N_i m_n + Z_i m_p - B(N_i, Z_i) \quad (43)$$

with vacuum binding energy $B(N_i, Z_i)$. For nuclei they are taken from the atomic mass evaluation AME2012 [41] if they are experimentally known. For other nuclei the values of the DZ10 [42] mass formula are assumed. For the two-nucleon resonance states we have $B(N_i, Z_i) = 0$.

The scalar potential

$$S_i = \Gamma_{i\sigma} A_\sigma - \Delta m_i \quad (44)$$

of a particle i and the vector potential

$$V_i = \Gamma_{i\omega} A_\omega + \Gamma_{i\rho} A_\rho + V_i^{(r)} \quad (45)$$

appearing in equation (42) receive contributions from the meson fields with strengths A_m ($m = \sigma, \omega, \rho$) and couplings Γ_{im} which are a product

$$\Gamma_{im} = g_{im} \Gamma_m(n_B) \quad (46)$$

of constant scaling factors g_{im} and functions $\Gamma_m(n_B)$ of the total baryon number density

$$n_B = \sum_i B_i n_i. \quad (47)$$

We use $g_{i\sigma} = g_{i\omega} = B_i$ and $g_{i\rho} = B_i - 2Q_i$ for nucleons and clusters, i.e. nucleons bound in nuclei couple with the same strength to mesons as free nucleons. Obviously, $g_{e\sigma} = g_{e\omega} = g_{e\rho} = 0$ for electrons. The functional dependence of the couplings Γ_m has the form as given in Ref. [27] with the well-calibrated DD2 parametrization that was obtained from a fit to finite nuclei. The mass shifts Δm_i contributing to the mean-field contribution in the scalar potential S_i are medium-dependent properties

determined by the Pauli blocking. They are specified in detail in appendix B. For nucleons and electrons $\Delta_i = 0$.

The contributions to the grand canonical potential density

$$\omega_{gc}(T, \mu_n, \mu_p, \dots) = \sum_i \omega_i^{(\text{qp})} + \omega^{(\text{int})} \quad (48)$$

are those of independent quasiparticles

$$\begin{aligned} \omega_i^{(\text{qp})} & \quad (49) \\ &= -g_i \frac{T}{\sigma_i} \int \frac{d^3k}{(2\pi)^3} \ln \left\{ 1 + \sigma_i \exp \left[-\frac{E_i(k) - \mu_i}{T} \right] \right\} \end{aligned}$$

(with $\sigma_i = +1$ for fermions and $\sigma_i = -1$ for bosons) and that of the interaction

$$\begin{aligned} \omega^{(\text{int})} &= \frac{1}{2} m_\sigma^2 A_\sigma^2 - \frac{1}{2} m_\omega^2 A_\omega^2 - \frac{1}{2} m_\rho^2 A_\rho^2 \\ &\quad - \sum_i V_i^{(r)} n_i \end{aligned} \quad (50)$$

with rearrangement potentials $V_i^{(r)}$ which also appear in the vector potentials (45). They are required in order to have a thermodynamic consistent theory (see below).

The quantity g_i in equation (49) denotes the degeneracy factor of a particle i . For nucleons and light nuclei we have $g_p = g_n = 2$ and $g_{(1,1)} = 3$ (${}^2\text{H}$), $g_{(2,1)} = g_{(1,2)} = 2$ (${}^3\text{H}$, ${}^3\text{He}$), $g_{(2,2)} = 1$ (${}^4\text{He}$). For heavier nuclei, $g_{(N,Z)}$ depends on the temperature T due to the excitation of states in a warm medium, see appendix C. The effective temperature dependent degeneracy factors for the two-nucleon resonance states are determined from the consistency relations as discussed in Ref. [31].

The single-quasiparticle number densities n_i in equations (47) and (50) are given by

$$n_i = g_i \int \frac{d^3k}{(2\pi)^3} f_i(E_i, \mu_i, T) \quad (51)$$

with the conventional distribution functions

$$f_i(E_i, \mu_i, T) = \left[\exp \left(\frac{E_i - \mu_i}{T} \right) + \sigma_i \right]^{-1} \quad (52)$$

for fermions and bosons. Note that the grand canonical potential density (48) is a functional of temperature and chemical potentials even though the densities n_i appear explicitly in the definition of the individual contributions to ω_{gc} . The form (51) is consistent with the thermodynamic definition

$$n_i = - \left. \frac{\partial \omega_{gc}}{\partial \mu_i} \right|_{T, \mu_j \neq \mu_i} \quad (53)$$

if the rearrangement potentials are defined correctly. For nuclei with mass number $A > 4$ it is sufficient to use Maxwell-Boltzmann statistics, corresponding to the limit $\sigma_i \rightarrow 0$ in equations (49) and (52). Furthermore we use for

these nuclei the nonrelativistic approximation (including rest mass)

$$E_i(k) = \frac{k^2}{2(m_i - S_i)} + m_i - S_i + V_i \quad (54)$$

of the quasiparticle energies (42). Then we find

$$\omega_i^{(\text{qp})} = -T n_i = -\frac{g_i T}{\lambda_i^3} \exp \left(\frac{\mu_i - V_i + S_i}{T} \right) \quad (55)$$

with the thermal wavelengths $\lambda_i = \sqrt{2\pi/[(m_i - S_i)T]}$.

The strengths A_m of the meson fields appear as auxiliary quantities in the grand canonical potential density ω_{gc} . They are obtained from the (trivial) fields equations

$$m_m^2 A_m = \Gamma_m^2 n_m \quad (56)$$

that are found with the help of the Euler-Lagrange equations. The source densities n_m in equation (56) are given by

$$n_\omega = \sum_i g_{i\omega} n_i \quad (57)$$

$$n_\rho = \sum_i g_{i\rho} n_i \quad (58)$$

$$n_\sigma = \sum_i g_{i\sigma} n_i^{(s)} \quad (59)$$

with the scalar quasiparticle number densities

$$\begin{aligned} n_i^{(s)} & \quad (60) \\ &= g_i \int \frac{d^3k}{(2\pi)^3} f_i(E_i, \mu_i, T) \frac{m_i - S_i}{\sqrt{k^2 + (m_i - S_i)^2}}. \end{aligned}$$

This integral reduces to

$$n_i^{(s)} = n_i \left(1 - \frac{3}{2} \frac{T}{m_i - S_i} \right) \quad (61)$$

for heavy nuclei with $A > 4$ in the above-mentioned approximation.

The rearrangement potentials

$$V_i^{(r)} = B_i U^{(\text{meson})} + U_i^{(\text{mass})} \quad (62)$$

include the standard meson contribution

$$U^{(\text{meson})} = \Gamma'_\omega A_\omega n_\omega + \Gamma'_\rho A_\rho n_\rho - \Gamma'_\sigma A_\sigma n_\sigma \quad (63)$$

with derivatives $\Gamma'_m = d\Gamma_m/dq_V$ of the couplings and a term

$$U_i^{(\text{mass})} = \sum_j \frac{\partial \Delta m_j}{\partial n_i} n_j^{(s)} \quad (64)$$

related to the medium dependent mass shifts of the quasiparticles.

The entropy density is obtained from the thermodynamic definition

$$\begin{aligned}
 s &= - \left. \frac{\partial}{\partial T} \omega_{gc} \right|_{\mu_i} \quad (65) \\
 &= - \sum_i g_i \int \frac{d^3k}{(2\pi)^3} [f_i \ln(f_i) \\
 &\quad + \sigma_i (1 - \sigma_i f_i) \ln(1 - \sigma_i f_i)] \\
 &\quad - \sum_i \left[\frac{d \ln(g_i)}{dT} \omega_i^{(qp)} + \frac{\partial \Delta m_i}{\partial T} n_i^{(s)} \right]
 \end{aligned}$$

with two non-standard terms in addition to the conventional contribution. They are caused by the temperature dependence of the degeneracy factors and of the mass shifts. Further thermodynamic quantities such as the free energy density

$$f = \omega_{gc} + \sum_i \mu_i n_i \quad (66)$$

and the internal energy density

$$u = f + Ts \quad (67)$$

are immediately obtained from the grand canonical potential density ω_{gc} which is just the negative pressure p .

We study dense matter in chemical equilibrium and assume that all reactions that change the chemical composition of the system, except those mediated by the weak interaction, are equilibrated. As a result, the chemical potentials μ_i of all particles are not independent. Because there are three independent conserved charges (baryon number, charge number, lepton number) the corresponding three chemical potentials μ_B, μ_Q, μ_L are sufficient to specify the chemical potentials

$$\mu_i = B_i \mu_B + Q_i \mu_Q + L_i \mu_L \quad (68)$$

for all constituents. In nuclear matter, leptons are not considered and the leptonic contribution in (68) can be ignored. In this case, the total charge number density

$$n_Q = \sum_i Q_i n_i \geq 0 \quad (69)$$

is related to the asymmetry by

$$n_Q = \frac{1 - \delta}{2} n_B. \quad (70)$$

In stellar matter, there is the additional condition of charge neutrality $n_Q = 0$ that determines the (electronic) lepton chemical potential μ_L for given asymmetry

$$\delta = 1 - 2 \frac{n_L}{n_B} \quad (71)$$

of the matter with

$$n_L = \sum_i L_i n_i = n_e \geq 0 \quad (72)$$

when only electrons are considered. Thus, there are only two independent chemical potentials μ_B and μ_Q .

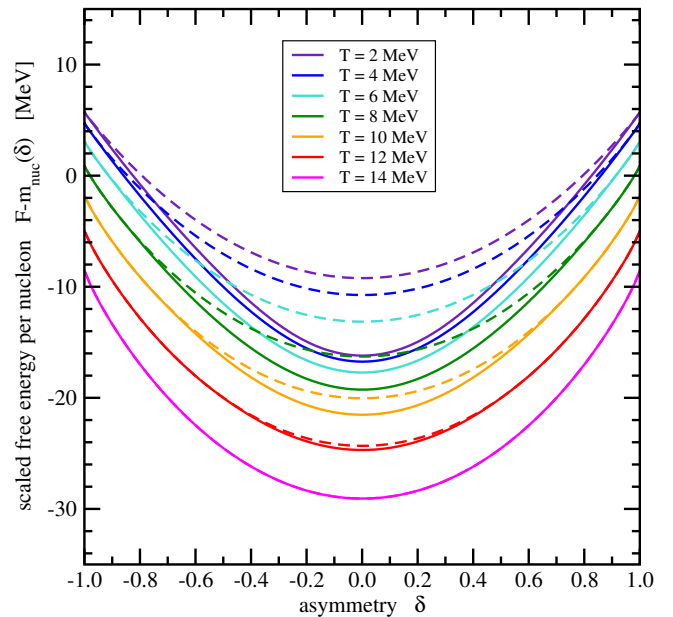


Fig. 5. Free energy per nucleon F corrected for the trivial mass contribution $m_{\text{nuc}}(\delta)$, Eq. (75), as a function of the asymmetry δ in nuclear matter at the critical baryon density n_{crit} of the DD2 parametrization for different temperatures T without (dashed lines) and with (full lines) liquid-gas phase transition without cluster formation.

3.2 Symmetry energy in the gRDF approach

The density dependence of the symmetry energy below nuclear saturation density will be affected by two reasons: the definition of the symmetry energy and the occurrence of spatial inhomogeneities be it a phase transition or the appearance of finite size clusters. In this subsection, the effects will be presented as they appear by applying the gRDF model. For the DD2 parametrization, used in the present calculations, the saturation density of symmetric nuclear matter at zero temperature is $n_{\text{sat}} \approx 0.149 \text{ fm}^{-3}$ [27]. Above this density, no effects from the liquid-gas phase transition or cluster formation occur and the usual results for the density dependence of the symmetry energy are recovered. Hence, we limit the range in the figures to sub-saturation densities.

3.2.1 Nuclear matter

In nuclear matter, only nucleons are considered as constituent particles but not leptons. There is a liquid-gas phase transition at densities below the nuclear saturation density and below the critical temperature $T_{\text{crit}} = 13.724 \text{ MeV}$ of symmetric nuclear matter in the gRDF approach. In the present subsection no clusters are considered in contrast to Ref. [27] because the effects of the liquid-gas phase transition on the symmetry energy are the main focus. The formation of clusters at low densities and low temperatures affects the main features of the phase transition only slightly since clusters appear in a

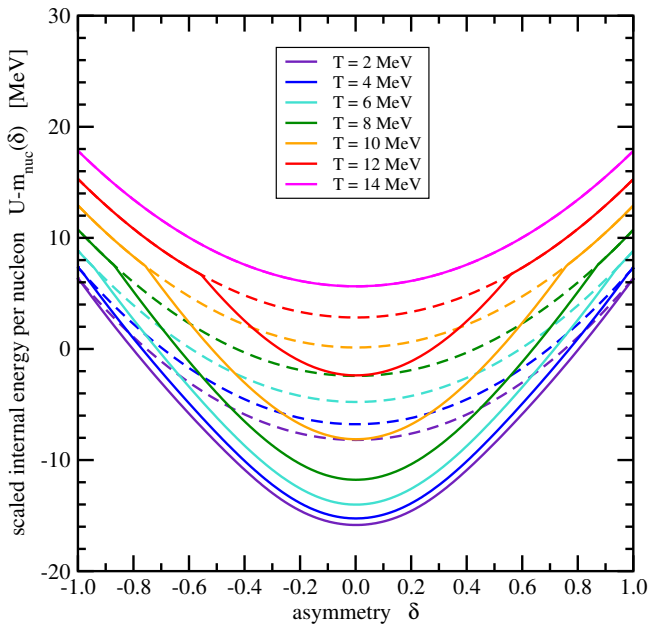


Fig. 6. Internal energy per nucleon U corrected for the trivial mass contribution $m_{\text{nuc}}(\delta)$ as a function of the asymmetry δ in nuclear matter at the critical baryon density n_{crit} of the DD2 parametrization for different temperatures T without (dashed lines) and with (full lines) liquid-gas phase transition without cluster formation.

substantial amount only for densities, temperatures and asymmetries that lie inside the coexistence region of the liquid-gas phase transition.

However, the liquid-gas phase transition will change the dependence of the free energy per nucleon

$$F(T, n_B, \delta) = \frac{1}{n_B} f(T, n_B, \delta) \quad (73)$$

on the asymmetry δ for constant temperature T and baryon density n_B . The quantity f is the free energy density in the gRDF model, equation (66). Similarly, the internal energy per nucleon is defined as

$$U(T, n_B, \delta) = \frac{1}{n_B} u(T, n_B, \delta) \quad (74)$$

with the internal energy density u of equation (67).

The dependence of F and U on δ for constant critical baryon density $n_B^{(\text{crit})} = 0.04515 \text{ fm}^{-3}$ is depicted in figures 5 and 6, respectively, for various temperatures. The trivial δ dependent contribution of the rest masses

$$m_{\text{nuc}}(\delta) = \frac{1 + \delta}{2} m_n + \frac{1 - \delta}{2} m_p \quad (75)$$

has been subtracted in these figure for clarity. Dashed lines show the results assuming uniform nuclear matter without a phase transition. There is a smooth variation of the energies, symmetric in δ , with an almost perfect quadratic dependence. With the liquid-gas phase transition, we observe a reduction of the energies that is most

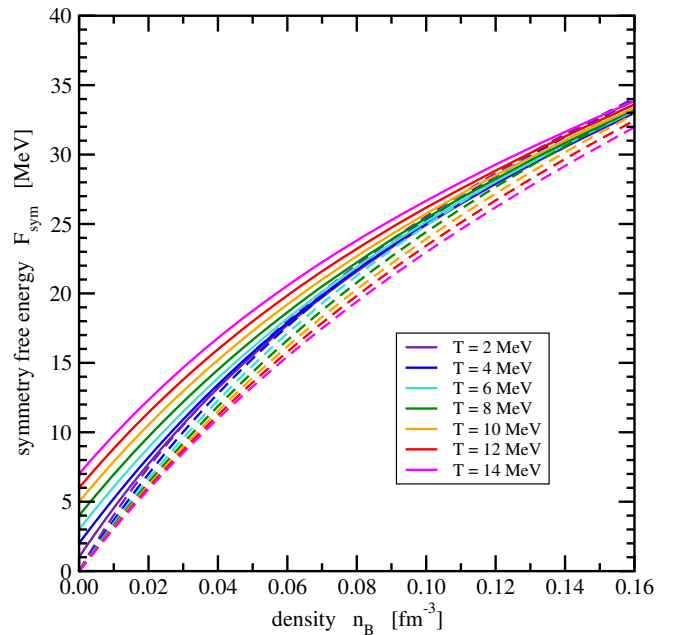


Fig. 7. Symmetry free energy F_{sym} in uniform nuclear matter without liquid-gas phase transition and without cluster formation as a function of the baryon density n_B for various temperatures in the second-derivative definition (dashed lines) and the finite difference definition (full lines).

pronounced at symmetric nuclear matter. This reduction is larger for lower temperatures and vanishes for $T \geq T_{\text{crit}}$. Thus it is absent in the lines for $T = 14 \text{ MeV}$. The free energy per nucleon is a convex function of δ as required by thermodynamical stability. But the internal energy per nucleon U exhibits a structure clearly indicating the transition to the region of coexisting phases at small asymmetries. The width of this zone increases with decreasing temperature. It is also evident from these two figures that the quadratic dependence on δ does not hold for large $|\delta|$. There, it is closer to a linear dependence as observed already for the minimum curves in figure 2 for nuclei.

As mentioned in subsection 2.2.1, the symmetry free energy $F_{\text{sym}}(T, n_B)$ can be defined by a second derivative as in equation (25) or by a finite difference as

$$F_{\text{sym}}(n_B) = \frac{1}{2} [F(n_B, +1) - 2F(n_B, 0) + F(n_B, -1)] \quad (76)$$

Similarly, we have the symmetry internal energy (26) from a second derivative and the finite difference form

$$U_{\text{sym}}(n_B) = \frac{1}{2} [U(n_B, +1) - 2U(n_B, 0) + U(n_B, -1)] . \quad (77)$$

The differences between these definition are shown in figures 7 and 8 for uniform nuclear matter without the liquid-gas phase transition. The agreement of the two definitions are very good for the symmetry internal energy U_{sym} at

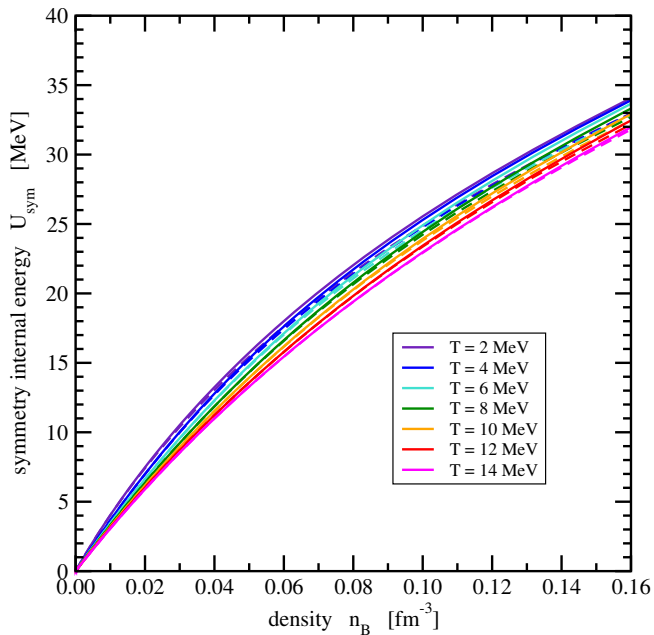


Fig. 8. Symmetry internal energy U_{sym} in uniform nuclear matter without liquid-gas phase transition and without cluster formation as a function of the baryon density n_B for various temperatures in the second-derivative definition (dashed lines) and the finite difference definition (full lines).

all densities. But for the symmetry free energy larger systematic deviations are seen that can reach several MeV. The symmetry free energy $F_{\text{sym}}(T, n_B)$ approaches a finite value for $n_B \rightarrow 0$ that rises with the temperature T . It is due to the entropy differences with

$$\lim_{n_B \rightarrow 0} F_{\text{sym}}(T, n_B) = T \ln 2. \quad (78)$$

In contrast to that, the symmetry internal energy U_{sym} always approaches zero in this limit.

Now let us turn to the calculation with the liquid-gas phase transition and perform the same comparison of the two definitions. The corresponding results are depicted in figures 9 and 10 using logarithmic scales on the axes for a better representation. A vast difference between the two symmetry energy definitions is found in the region of the coexisting phases. Only in the range of uniform nuclear matter the two approaches give similar results with systematically lower values of the symmetry free energy when the derivative definition is used. The finite difference formulas (76) and (77) give reasonable quantitative results for the symmetry free energy and the symmetry internal energy for all densities reflecting the difference in energies between symmetric nuclear matter and pure neutron/proton matter. The second derivative definitions (25) and (26) however produce huge values of the symmetry energy in the phase coexistence region, in particular at higher baryon densities close to the transition to uniform nuclear matter. The finite difference formula for the symmetry energy gives a better impression about the variation of the energy per particle with the isospin variation.

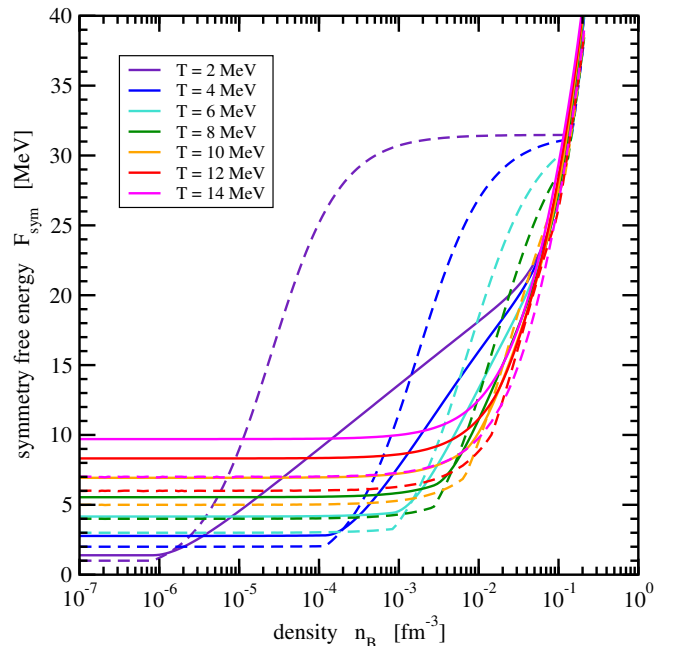


Fig. 9. Symmetry free energy F_{sym} in nuclear matter with liquid-gas phase transition but without cluster formation as a function of the baryon density n_B for various temperatures in the second-derivative definition (full lines) and the finite difference definition (dashed lines).

Hence, we will use this definition in the following discussion.

In figures 11 and 12, the symmetry free energy and the symmetry internal energy without and with liquid-gas phase transition are depicted in a linear scale for the symmetry energies employing the finite difference formula. The effect of the phase transition is easily discerned. We emphasize that the values at low densities are a result of the separation of phases and not due to cluster formation that is not taken into account in the nuclear matter calculations. The effects of clusters will be considered only in the next subsection. Due to the different low-density limits, the effect on the symmetry internal energy is more pronounced. A particular interesting case is the low-density behavior of the symmetry energies for zero temperature that is depicted in these figure, too. Both the symmetry free and symmetry internal energy approach a finite value in this exceptional situation with $n_B \rightarrow 0$. The limiting value is just the binding energy $B_{\text{sat}} \approx 16$ MeV of nuclear matter at saturation.

3.2.2 Stellar matter

In the calculation of stellar matter properties the full set of constituents in the gRDF model is used, i.e. nucleons, electrons, and all nuclei with $A \leq 350$. In order to follow the evolution of the chemical composition, we introduce

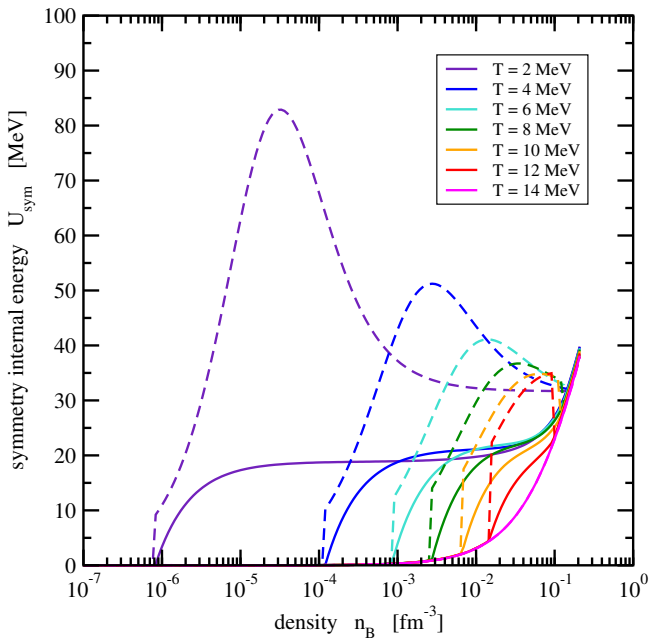


Fig. 10. Symmetry internal energy U_{sym} in nuclear matter with liquid-gas phase transition but without cluster formation as a function of the baryon density n_B for various temperatures in the second-derivative definition (full lines) and the finite difference definition (dashed lines).

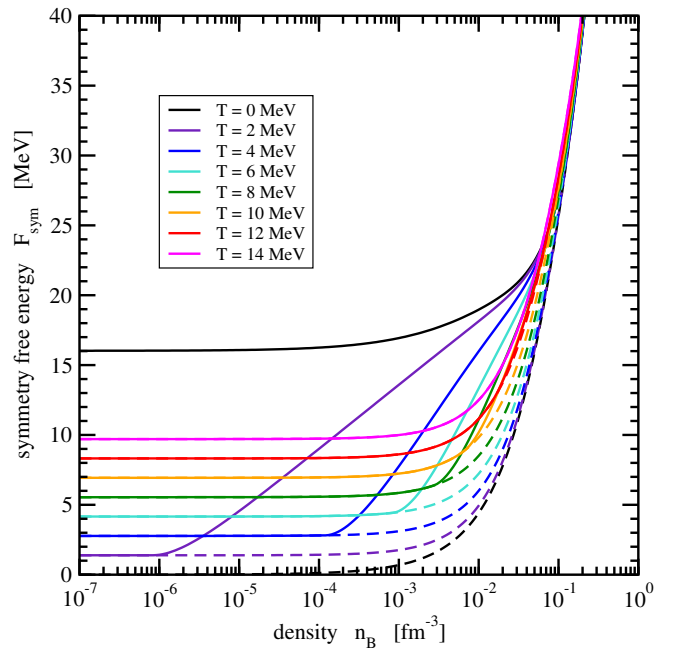


Fig. 11. Symmetry free energy F_{sym} in nuclear matter without cluster formation, without (dashed lines) and with (full lines) liquid-gas phase transition, as a function of the baryon density n_B for various temperatures using the finite difference definition of the symmetry free energy.

the particle fractions

$$X_{\text{light}} = \frac{1}{n_B} \sum_{i \in \mathcal{S}_{\text{light}}} A_i n_i \quad (79)$$

of the light clusters (set $\mathcal{S}_{\text{light}} = \{^2\text{H}, ^3\text{H}, ^3\text{He}, ^4\text{He}\}$) and

$$X_{\text{heavy}} = \frac{1}{n_B} \sum_{i \in \mathcal{S}_{\text{heavy}}} A_i n_i \quad (80)$$

of the heavy clusters (set $\mathcal{S}_{\text{heavy}} = \{(N_i, Z_i) | A_i > 4\}$). In figure 13 the quantities X_{light} and X_{heavy} are shown as a function of the baryon number density n_B for various temperatures in stellar matter with asymmetry $\delta = 0$. At low densities, light clusters are the prevailing species. Heavy clusters dominate the composition at higher densities as long as the temperature is not too high. When the density approaches nuclear saturation density, all cluster dissolve as expected. Thus the model accounts for the Mott effect. It is due to the mass shifts of clusters in the gRDF model, which are given in appendix B including the electron screening in the Wigner-Seitz approximation. It is a more microscopic alternative to the often used excluded volume mechanism to suppress the occurrence of nuclei in a dense medium. The effective degeneracy factors accounting for internal excitations are given in appendix C.

More information on the chemical composition is given by the average mass numbers

$$\langle A \rangle_{\text{light}} = \frac{\sum_{i \in \mathcal{S}_{\text{light}}} A_i n_i}{\sum_{i \in \mathcal{S}_{\text{light}}} n_i} \quad (81)$$

and

$$\langle A \rangle_{\text{heavy}} = \frac{\sum_{i \in \mathcal{S}_{\text{heavy}}} A_i n_i}{\sum_{i \in \mathcal{S}_{\text{heavy}}} n_i} \quad (82)$$

of the light and of the heavy component that are depicted in figure 14. At very low densities, the cluster composition is mainly given by light nuclei, i.e. ^2H in the light and ^6Li in the heavy component. With increasing density, the average mass number rises. The light clusters turn into α particles and heavy cluster become substantially more massive but $\langle A \rangle_{\text{heavy}}$ does not exceed 200 in the present gRDF model for $\delta = 0$. At low temperatures, shell effects in the nuclear binding energies cause the particular structure of the average mass number and charge number evolution with the density. At higher temperatures, these effects are washed out. The density range where clusters give an important contribution to the chemical composition shrinks with increasing temperature. Beyond $T \approx 10$ MeV, heavy clusters quickly disappear.

Electrons are an essential component in stellar matter because they guarantee the charge neutrality of the system and screen the Coulomb interaction at high densities. They contribute in a sizeable amount to the thermodynamic quantities, in particular to the energies and pressure. Because the electronic contribution is not symmetric in the asymmetry parameter δ , the isospin symmetry as it appears in nuclear matter does not hold any more. This is clearly seen in figures 15 and 16 which show with dashed lines the variation of the free energy F and internal energy U per nucleon with δ for stellar matter at a constant baryon density $n_B = 0.002 \text{ fm}^{-3}$. The contribution of the

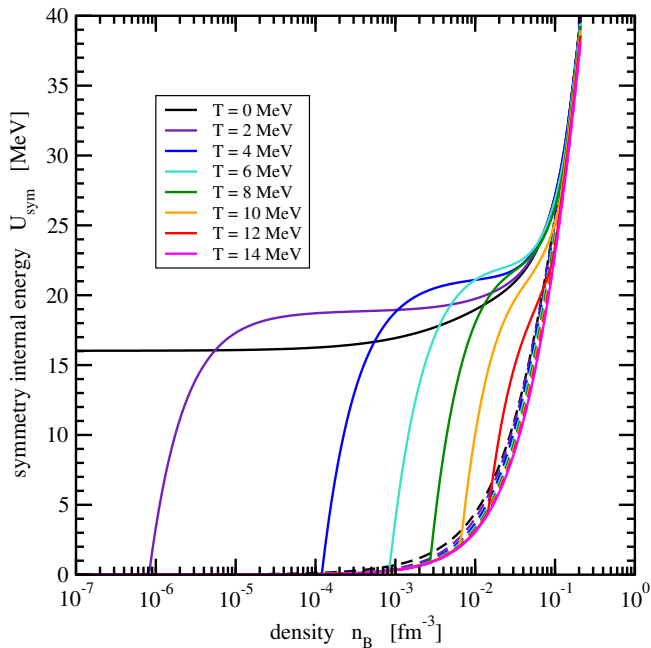


Fig. 12. Symmetry internal energy U_{sym} in nuclear matter without cluster formation, without (dashed lines) and with (full lines) liquid-gas phase transition, as a function of the baryon density n_B for various temperatures using the finite difference definition of the symmetry internal energy.

electrons leads to an increase of the energies in proton rich matter.

Similarly as in the Bethe-Weizsäcker formula (2) the effect of the Coulomb interaction and the electronic contribution has to be removed from the energies (apart from the trivial neutron-proton mass difference effect) in order to obtain values for the symmetry energies that are comparable to those of nuclei or nuclear matter. For this purpose, we subtract the contribution of the electrons from the total thermodynamical quantities. This is easily carried out in the formulation of the gRDF model in subsection 3.1. The second correction concerns the Coulomb contribution to the binding energies of the nuclei. In the medium, the Coulomb energy is already partially screened as described by the energy shift $\Delta E_i^{(\text{Coul})}$ in equation (106). Thus we have to add only the remaining Coulomb shift that is required to obtain binding energies of nuclei without the Coulomb interaction. This is performed in the calculation for all nuclei with the proper weights proportional to their densities. The energies modified in this manner are plotted in figures 15 and 16 with full lines. We observe an almost perfect symmetry with respect to $\delta = 0$. The effect of the cluster formation in the medium on the shape becomes more obvious after the electron and Coulomb corrections were considered. For low temperatures there is a considerable reduction of the energies for small values of δ . For temperatures above $T \approx 6$ MeV the effect is almost disappearing as expected from the information on the chemical composition in figures 13 and 14 as well as from the occurrence of the phase transition in figures 11 and 12. The full

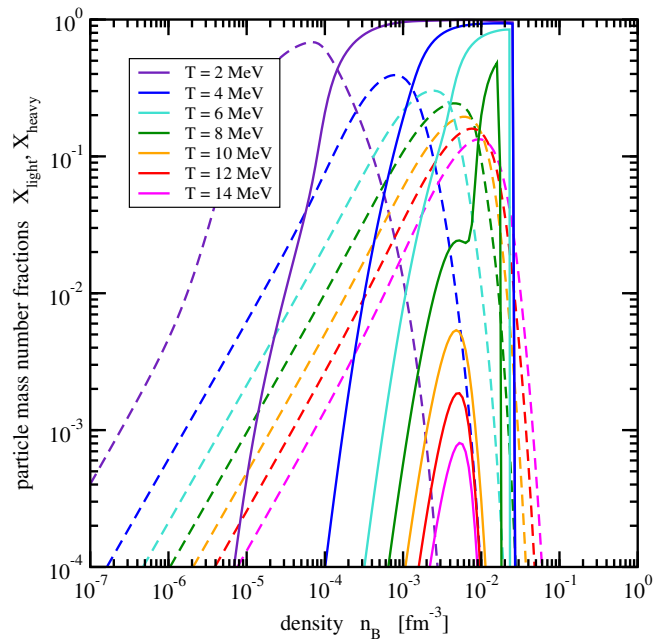


Fig. 13. Mass number fractions of light (dashed lines) and heavy nuclei (full lines) in stellar matter with asymmetry $\delta = 0$ for different temperature T as a function of the baryon number density n_B .

lines in figures 15 and 16 exhibit the same trend that was already depicted in figure 12 of Ref. [27] where only light clusters were included in the theoretical model. Due to the inclusion of the heavy nuclei in the current calculation, the minimum is rounded and less triangular shaped.

Using the finite-difference definition of the symmetry energy, the dependence of the symmetry free and symmetry internal energies as a function of the baryon density are obtained without and with the electron and Coulomb corrections. The results are displayed in figures 17 and 18. The differences between the uncorrected and corrected results are clearly visible. With the correction, the symmetry energies are too large because of the larger variation of the energies with δ for constant baryon density due to the electronic contribution. Only at low densities both calculations will merge since the charge densities and Coulomb shifts become very small. We also notice that the clustering in dense stellar matter leads to reduced symmetries as compared to those in nuclear matter with liquid-gas phase transition. This is true both in absolute value and in the extension of the density range. Comparing the results in figures 17 and 18 with those in figure 13 (a) and 14 (a) of Ref. [27] we observe that the occurrence of heavy nuclei increases the symmetry energies at low temperatures due to their larger binding energies as those of the light clusters.

Cluster formation was not included in the calculation of the symmetry energy in nuclear matter with liquid-gas phase transition. In contrast, no phase transition construction was applied to the presented results for stellar matter in order to expose the effect of clustering as clearly as pos-

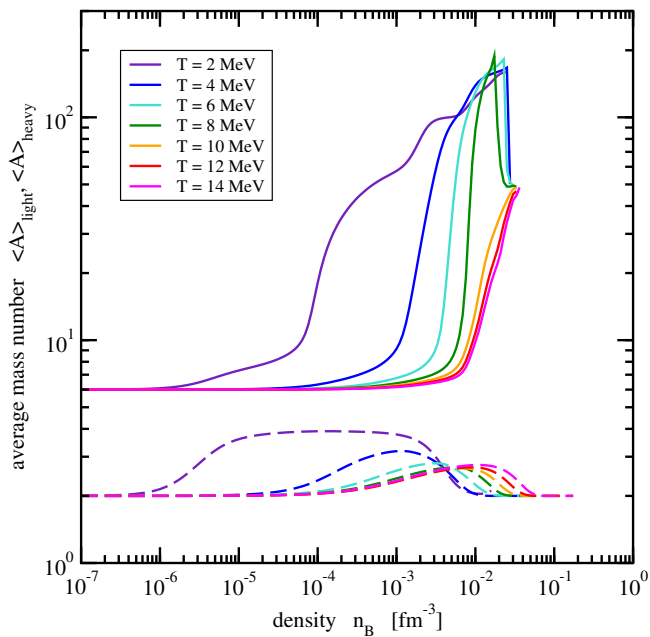


Fig. 14. Average mass number of light (dashed lines) and heavy nuclei (full lines) in stellar matter with asymmetry $\delta = 0$ for different temperature T as a function of the baryon number density n_B .

sible. As a consequence, some non-monotonic behavior of the curves in figures 17 and 18 is observed at lower temperatures. This is caused by the sudden disappearance of the clusters with increasing density. The effect would vanish when the phase transition was fully accounted for. The phase transition construction in stellar matter is somewhat different as in nuclear matter due to the additional conserved charge, the lepton number, and the charge neutrality condition. See appendix A for more details. However, at the relevant temperatures and densities, a more refined calculation should take into account the appearance of "pasta" structures with complicated spatial density distributions that smoothen the transition from matter with clusters to homogeneous matter. A liquid-gas type phase transition construction can only roughly represent this transition. We leave the full treatment to a future publication in the context of providing a global equation of state table of stellar matter for astrophysical applications.

4 Conclusions

The symmetry energy is a valuable concept to characterize the dependence of the energy on the isospin asymmetry of a system. However, due to the different definitions of this quantity and the specific thermodynamic conditions of the system, a comparison of the symmetry energies derived from different sources needs a careful consideration of possible discrepancies. Besides finite nuclei, the symmetry energy of dense matter as a function of the density

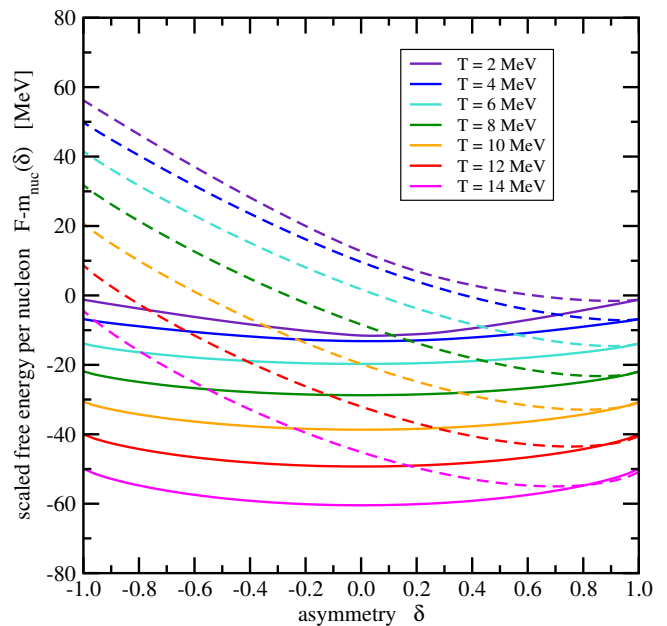


Fig. 15. Free energy per nucleon F corrected for the trivial mass contribution $m_{\text{nuc}}(\delta)$ as a function of the asymmetry δ in stellar matter at a baryon density of $n_B = 0.002 \text{ fm}^{-3}$ for different temperatures T without (dashed lines) and with (full lines) the Coulomb correction.

is of particular interest in theoretical and experimental investigations.

In the present work, the symmetry free energy and symmetry internal energy of nuclear matter and of stellar matter were extracted from theoretical calculations employing a generalized relativistic density functional approach, which allows to describe the appearance of the liquid-gas phase transition or the formation and dissolution of finite-size clusters. In stellar matter, corrections for the existence of electrons and for the action of the electromagnetic interaction are required in order to extract the pure nuclear symmetry energy.

Results of various definitions for the symmetry energy were presented. In systems with phase transition or cluster degrees of freedom, substantial differences for the symmetry energy are found by comparing the definitions using second derivatives or finite differences. The latter approach, which compares symmetric matter with pure neutron and proton matter, seems to give more reasonable sizes of the symmetry energy. The occurrence of spatially inhomogeneous density distributions causes an increase of the symmetry energies at low densities, in particular at low temperatures. This is in strong contrast to theoretical calculations assuming uniform uncorrelated matter.

The comparison of experimentally determined symmetry energies with those extracted from theoretical calculations is neither straightforward nor necessarily direct. This topic deserves a more extended discussion but it is beyond the scope of the present paper. However, a few remarks are in order. In most investigations of heavy-ion collisions, theoretical model simulations are utilized in or-

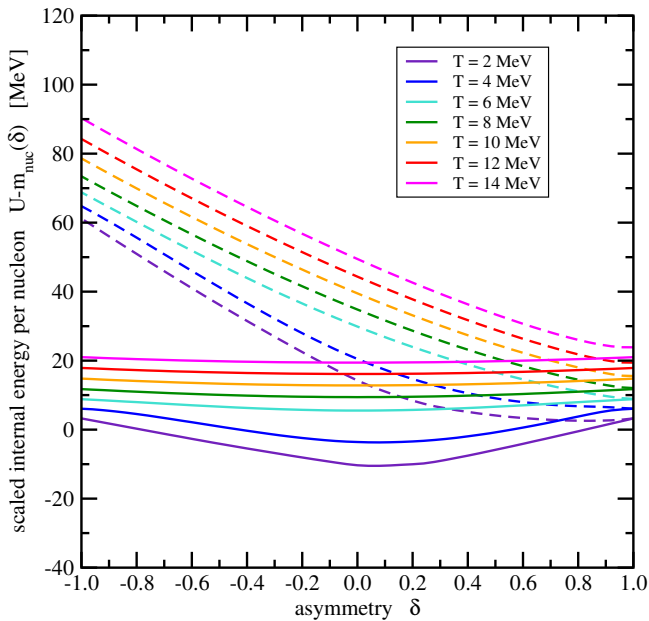


Fig. 16. Internal energy per nucleon U corrected for the trivial mass contribution $m_{\text{nuc}}(\delta)$ as a function of the asymmetry δ in stellar matter at a baryon density of $n_B = 0.002 \text{ fm}^{-3}$ for different temperatures T without (dashed lines) and with (full lines) the Coulomb correction.

der to describe experimental observables that are sensitive to the isospin asymmetry. As a result the isovector dependence of the interaction of the underlying model or energy density functional is explored. It is connected to the density dependence of the symmetry energy for homogeneous Coulomb-less nuclear matter, which is conveniently encoded in quantities like J , L , or K_{sym} for an easy comparison of models. This does not mean that clusterization effects are not accounted for in the experiments or that the extracted values of the coefficients J , L , or K_{sym} represent the physical symmetry energy. Only in few cases, e.g. in Ref. [24], it is attempted to extract a symmetry energy directly without the need to consider an intermediate simulation with a theoretical model. In these cases, effects of clusterization as they appear in the physical system under study will naturally affect the extracted symmetry energy. The considerations of the present paper apply to the comparison of symmetry energies that were directly determined in experiments to those of indirect approaches employing, e.g., numerical simulations of heavy-ion collisions.

This work was supported by the Helmholtz Association (HGF) through the Nuclear Astrophysics Virtual Institute (VH-VI-417), by CompStar, a Research Networking Program of the European Science Foundation (ESF), by CompStar-POL and by the Helmholtz International Center for FAIR within the framework of the LOEWE program launched by the state of Hesse via the Technical University Darmstadt. D.B. was supported by NCN within the ‘‘Maestro’’ program under grant

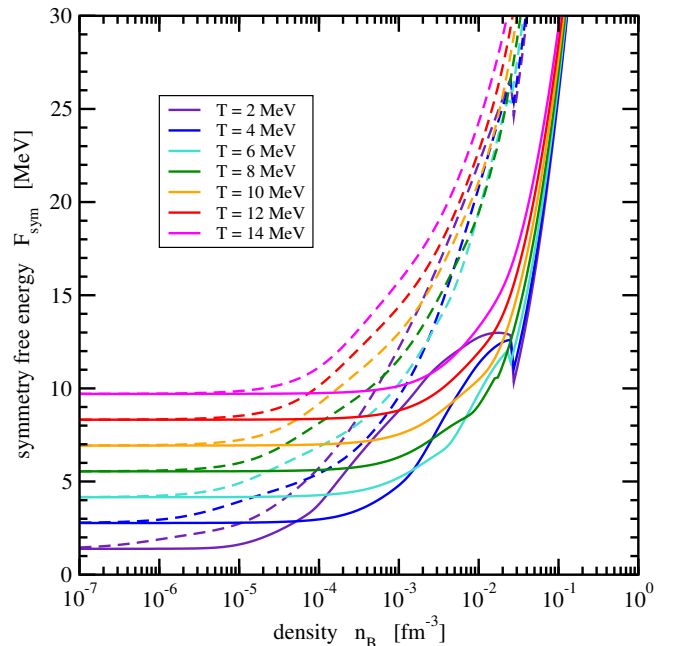


Fig. 17. Symmetry free energy F_{sym} in stellar matter without (dashed lines) and with (full lines) Coulomb and electron correction as a function of the baryon density n_B for various temperatures using the finite difference definition of the symmetry free energy.

No. DEC-2011/02/A/ST2/00306 and by RFBR under grant No. 11-02-01538-a.

A Liquid-gas phase transition in dense matter

The thermodynamic state of dense matter is completely determined when the independent variables, i.e. the temperature and the densities of the conserved charges, are chosen. It can be found by a global minimization of the free energy density f . In some regions of the parameter space, dense matter will separate into coexisting phases. The cases of nuclear matter and stellar matter have to be distinguished for the construction of the phase transition, which is briefly presented in the following. A more detailed discussion of the phase transition construction with the isospin degree of freedom and the reduction from a general Gibbs construction to the simpler Maxwell construction can be found in Ref. [52].

A.1 Nuclear matter

In this case, the free energy density is a function of the independent variables T , n_B , and n_Q . For parameters n_B and $n_Q = (1 - \delta)n_B/2$ inside the binodals shown in figure 4 the correct free energy density is found by a linear interpolation of the free energy densities of the coexisting phases $\pi = 1$ and $\pi = 2$ at two points that lie on the binodal of given temperature T and have identical intensive

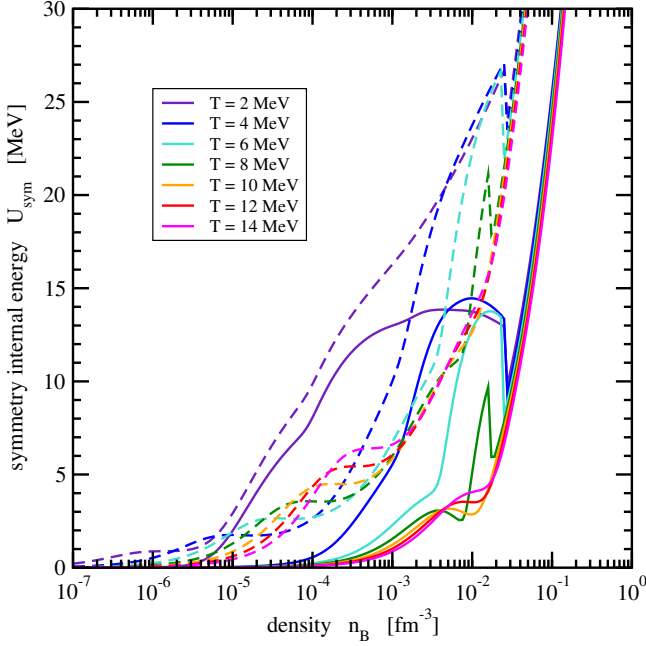


Fig. 18. Symmetry internal energy U_{sym} in stellar matter without (dashed lines) and with (full lines) Coulomb and electron correction as a function of the baryon density n_B for various temperatures using the finite difference definition of the symmetry internal energy.

variables, i.e. pressure

$$p^{(\text{coex})} = p(T, n_B^{(1)}, n_Q^{(1)}) = p(T, n_B^{(2)}, n_Q^{(2)}), \quad (83)$$

baryonic chemical potential

$$\mu_B^{(\text{coex})} = \mu_B(T, n_B^{(1)}, n_Q^{(1)}) = \mu_B(T, n_B^{(2)}, n_Q^{(2)}), \quad (84)$$

and charge chemical potential

$$\mu_Q^{(\text{coex})} = \mu_Q(T, n_B^{(1)}, n_Q^{(1)}) = \mu_Q(T, n_B^{(2)}, n_Q^{(2)}). \quad (85)$$

A practical way of finding the correct baryon ($n_B^{(1)}, n_B^{(2)}$) and charge ($n_Q^{(1)}, n_Q^{(2)}$) densities of the coexisting phases uses the modified thermodynamic potential

$$\tilde{f}_{\text{nuc}}(T, n_B, \mu_Q) = f(T, n_B, n_Q) - \mu_Q n_Q \quad (86)$$

that depends only on a single extensive-like variable, here the density n_B , apart from further intensive variables. The densities $n_B^{(1)}$ and $n_B^{(2)}$ are then found by a simple one-dimensional phase transition construction, e.g. the usual Maxwell construction, requiring

$$p^{(\text{coex})} = p(T, n_B^{(1)}, \mu_Q) = p(T, n_B^{(2)}, \mu_Q) \quad (87)$$

$$= n_B^2 \left. \frac{\partial (\tilde{f}_{\text{nuc}}/n_B)}{\partial n_B} \right|_{T, \mu_Q, n_B = n_B^{(\pi)}}$$

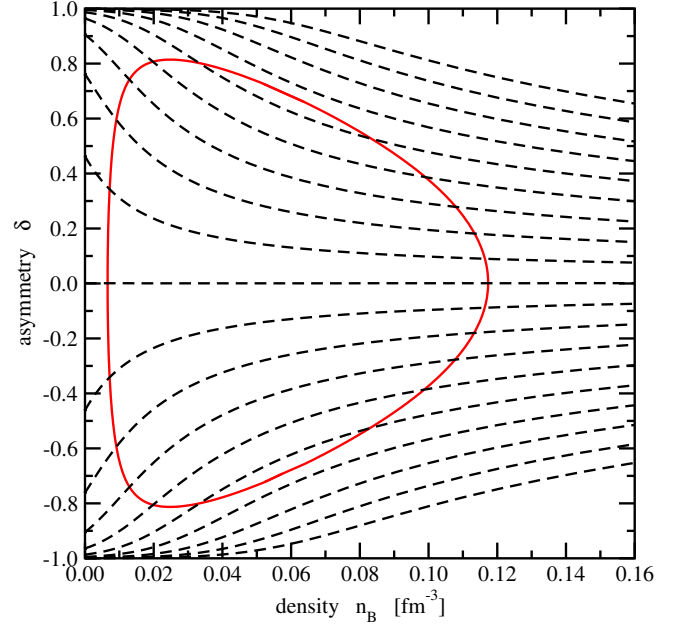


Fig. 19. Binodal (full red line) and lines of equal charge chemical potential μ_Q (dashed black lines, in steps of 10 MeV) for a temperature of $T = 10$ MeV in the gRDF model of nuclear matter without cluster formation in the asymmetry-density plane.

and

$$\mu_B^{(\text{coex})} = \mu_B(T, n_B^{(1)}, \mu_Q) = \mu_B(T, n_B^{(2)}, \mu_Q) \quad (88)$$

$$= \left. \frac{\partial \tilde{f}_{\text{nuc}}}{\partial n_B} \right|_{T, \mu_Q, n_B = n_B^{(\pi)}}$$

As a result, the charge densities

$$n_Q^{(\pi)} = n_Q(T, n_B^{(\pi)}, \mu_Q) = - \left. \frac{\partial \tilde{f}_{\text{nuc}}}{\partial \mu_Q} \right|_{T, n_B^{(\pi)}} \quad (89)$$

and entropy densities

$$s^{(\pi)} = s(T, n_B^{(\pi)}, \mu_Q) = - \left. \frac{\partial \tilde{f}_{\text{nuc}}}{\partial T} \right|_{\mu_Q, n_B^{(\pi)}} \quad (90)$$

of the two coexisting phases $\pi = 1, 2$ are obtained. In figure 19 the phase coexistence boundary and lines of constant charge chemical potential μ_Q are shown for $T = 10$ MeV using the gRDF model of nuclear matter. The points, where a line of constant μ_Q crosses the binodal, define the baryon densities, $n_B^{(1)}$ and $n_B^{(2)}$, and asymmetries of the coexisting phases. For all baryonic densities n_B inside the coexistence region, i.e. $n_B^{(1)} \leq n_B \leq n_B^{(2)}$, one has the corresponding charge density

$$n_Q(T, n_B, \mu_Q) = x_1 n_Q^{(1)} + x_2 n_Q^{(2)} \quad (91)$$

with

$$x_1 = \frac{n_B^{(2)} - n_B}{n_B^{(2)} - n_B^{(1)}} \quad (92)$$

and

$$x_2 = \frac{n_B - n_B^{(1)}}{n_B^{(2)} - n_B^{(1)}}. \quad (93)$$

Similarly, the free energy density

$$f(T, n_B, n_Q) = x_1 f^{(1)} + x_2 f^{(2)} \quad (94)$$

with

$$f^{(\pi)} = p^{(\text{coex})} + \mu_B^{(\text{coex})} n_B^{(\pi)} + \mu_Q^{(\text{coex})} n_Q^{(\pi)} \quad (95)$$

and other extensive-like thermodynamic quantities are calculated by a linear interpolation.

A.2 Stellar matter

In this case, there is an additional conserved charge, the total (electronic) lepton number. The free energy density $f(T, n_B, n_Q, n_L)$ depends on the temperature and three independent densities with three corresponding chemical potentials in general. However, the charge neutrality condition requires $n_Q = 0$. Instead of the modified free energy density $\tilde{f}_{\text{nuc}}(T, n_B, \mu_Q)$ as defined in equation (86) it is advantageous to introduce the modified free energy density

$$\tilde{f}_{\text{st}}(T, n_B, n_Q, \mu_L) = f(T, n_B, n_Q, n_L) - \mu_L n_L \quad (96)$$

of stellar matter. Setting $n_Q = 0$, hence considering a submanifold in the full parameter space, the construction of the phase transition can follow the same lines as in the case of nuclear matter by replacing n_Q and μ_Q in the previous subsection by n_L and μ_L .

B Medium dependent mass shifts of composite particles

The effective mass

$$m_i^{(\text{eff})} = N_i m_n + Z_i m_p - B(N, Z) - \Gamma_{i\sigma} A_\sigma + \Delta m_i \quad (97)$$

of a composite particle $i = (N, Z)$ in dense matter depends on the interaction with the σ meson field and the in-medium mass shift

$$\Delta m_i = \Delta E_i^{(\text{strong})} + \Delta E_i^{(\text{Coul})} \quad (98)$$

where we consider two contributions.

The strong mass shift $\Delta E_i^{(\text{strong})}$ includes the effect of the Pauli exclusion principle causing a blocking of nucleon states in the medium and the binding energy shift of nuclei due to the strong interaction. It is parametrized as a function of the temperature T and the effective density

$$n_i^{(\text{eff})} = \frac{2}{A_i} \left(N_i n_n^{(\text{tot})} + Z_i n_p^{(\text{tot})} \right) \quad (99)$$

with the total neutron and proton densities, $n_n^{(\text{tot})}$ and $n_p^{(\text{tot})}$, counting both nucleons that are free and bound inside clusters. In Ref. [27] these densities were replaced by

approximate values derived from the strengths of the ω and ρ meson fields resulting in a different form of the meson field equations and the rearrangement terms in the potentials. In the present approach the correct total proton and neutron densities are used. For light clusters (bound states and effective two-nucleon resonance states) we assume a product form

$$\Delta E_i^{(\text{strong})}(T, n_i^{(\text{eff})}) = f_i(n_i^{(\text{eff})}) \delta E_i^{(\text{Pauli})}(T) \quad (100)$$

where $\delta E_i^{(\text{Pauli})}(T)$ is given by equations (26) and (27) of Ref. [27] with $n = 0$ for two-nucleon and three/four-nucleon clusters, respectively. See also Refs. [50, 51] for an improved parametrization. The prefactor in (100) is given by the quadratic function

$$f_i(n_i^{(\text{eff})}) = n_i^{(\text{eff})} \left[1 + \frac{n_i^{(\text{eff})}}{2n_i^{(0)}(T)} \right] \quad (101)$$

with the reference density

$$n_i^{(0)}(T) = \frac{B(N_i, Z_i)}{\delta E_i^{(\text{Pauli})}(T)} \quad (102)$$

as in Ref. [27]. For heavy nuclei with $A > 4$ we use the pole form

$$\Delta E_i^{(\text{strong})}(T, n_i^{(\text{eff})}) = \frac{B(N_i, Z_i)}{1 - x_i} \quad (103)$$

with the parameter

$$x_i = \frac{n_i^{(\text{eff})}}{n_i^{(0)}} \quad (104)$$

for $x_i < 1$. It depends on the density scale

$$n_i^{(0)} = \frac{n_{\text{sat}}}{1 + 76/A_i} \quad (105)$$

with the saturation density n_{sat} of the DD2 parametrization. For $x_i \geq 1$ the particle i is no longer considered to exist in the medium.

The Coulomb contribution to the mass shift is taken from the Wigner-Seitz approximation

$$\Delta E_i^{(\text{Coul})} = E_i^{(\text{Coul})} \left[-\frac{3}{2} \frac{R_i}{R_i^{(e)}} + \frac{1}{2} \left(\frac{R_i}{R_i^{(e)}} \right)^3 \right] \quad (106)$$

with the Coulomb energy (4) and the electronic radius

$$R_i^{(e)} = \left(\frac{3Z_i}{4\pi n_e} \right)^{1/3} \quad (107)$$

that contains the electron density n_e which is assumed to be spatially uniform in the present description of dense matter.

C Effective degeneracy factors and density of states of nuclei

In a medium of finite temperature, not only the ground state of a nucleus can be populated but also excited states. As a consequence, there is a mixture of the nucleus in different excitation states in warm dense matter. The relative probabilities of the different excitation states can be found by applying the appropriate Boltzmann factors depending on the excitation energy ε . The effect can be summarized by introducing a temperature dependent degeneracy factor

$$g_{(N,Z)}(T) = g_{(N,Z)}^{(gs)} + \int_0^{E_{N,Z}^{(\max)}} d\varepsilon \varrho_{N,Z}^{(\text{exc})}(\varepsilon) \exp\left(-\frac{\varepsilon}{T}\right) \quad (108)$$

of a nucleus (N, Z) with the degeneracy of ground state $g_{(N,Z)}^{(gs)} = 2J_{N,Z}^{(gs)} + 1$ and a contribution of excited states containing the density of excited states $\varrho_{N,Z}^{(\text{exc})}(\varepsilon)$.

For the ground state spins $J_{N,Z}^{(gs)}$ experimental values are used as far as available. They are tabulated in the NUBASE2012 evaluation [53]. Otherwise we assume $J_{N,Z}^{(gs)} = 0$ for even-even nuclei, $J_{N,Z}^{(gs)} = 1$ for odd-odd nuclei, and $J_{N,Z}^{(gs)} = 1/2$ for the remaining nuclei.

Following Ref. [54], the density of excited states is assumed to have the form

$$\begin{aligned} \varrho_{N,Z}^{(\text{exc})}(\varepsilon) &= \frac{\sqrt{\pi}}{12} \left(\frac{a_{N,Z}^2}{4a_{N,Z}^{(n)}a_{N,Z}^{(p)}} \right)^{1/2} \frac{\exp\left(\beta_{N,Z}\varepsilon + \frac{a_{N,Z}}{\beta_{N,Z}}\right)}{(\beta_{N,Z}\varepsilon^3)^{1/2}} \\ &\times \frac{1 - \exp\left(-\frac{a_{N,Z}}{\beta_{N,Z}}\right)}{\left[1 - \frac{1}{2}\beta_{N,Z}\varepsilon \exp\left(-\frac{a_{N,Z}}{\beta_{N,Z}}\right)\right]^{1/2}}. \end{aligned} \quad (109)$$

Proper values for the function $\beta_{N,Z}(\varepsilon)$ are obtained by solving the equation

$$\left(\frac{a_{N,Z}}{\beta_{N,Z}}\right)^2 = a_{N,Z}\varepsilon \left[1 - \exp\left(-\frac{a_{N,Z}}{\beta_{N,Z}}\right)\right]. \quad (110)$$

that contains the level density parameter

$$a_{N,Z} = a_{N,Z}^{(n)} + a_{N,Z}^{(p)} \quad (111)$$

of a nucleus (N, Z) . For the level density parameters of the nucleons

$$a_{N,Z}^{(i)} = \frac{g_i}{2} \varrho_{N,Z}^{(i)} \frac{\pi^2}{3} \quad (112)$$

the free Fermi gas estimate

$$\varrho_{N,Z}^{(i)} = \frac{m_i k_{N,Z}^{(i)} V_{N,Z}}{2\pi^2} \quad (113)$$

is adopted with the nuclear volume

$$V_{N,Z} = \frac{4\pi}{3} r_0^3 (N + Z) \quad (114)$$

(using $r_0 = 1.4$ fm) and Fermi momenta

$$k_{N,Z}^{(n)} = \left(\frac{N}{V_{N,Z}} \frac{6\pi^2}{g_n}\right)^{1/3} \quad (115)$$

$$k_{N,Z}^{(p)} = \left(\frac{Z}{V_{N,Z}} \frac{6\pi^2}{g_p}\right)^{1/3} \quad (116)$$

at the neutron and proton Fermi energies.

The advantage of the form (109) is that the level density does not diverge for $\varepsilon \rightarrow 0$ but it remains finite with

$$\lim_{\varepsilon \rightarrow 0} \varrho_{N,Z}^{(\text{exc})}(\varepsilon) = \frac{\sqrt{2\pi}e}{12} a_{N,Z} \left(\frac{a_{N,Z}^2}{4a_{N,Z}^{(n)}a_{N,Z}^{(p)}}\right)^{1/2} \quad (117)$$

in contrast to many Fermi gas models following the original ideas of Bethe [55,56]. This is due to an explicit separation of the ground state contribution from the excited-states contribution in deriving the density of states by an inverse Laplace transformation. For high excitation energies, one finds $\beta_{N,Z} \rightarrow \sqrt{\varepsilon/a_{N,Z}}$ and the usual form

$$\varrho_{N,Z}^{(\text{exc})}(\varepsilon) \rightarrow \frac{\sqrt{\pi}}{12} \left(\frac{a_{N,Z}^2}{4a_{N,Z}^{(n)}a_{N,Z}^{(p)}}\right)^{1/2} \frac{\exp(2\sqrt{a_{N,Z}\varepsilon})}{a_{N,Z}^{1/4}\varepsilon^{5/4}} \quad (118)$$

of the Fermi gas model.

Because the density of states (109) is derived in a low-temperature approximation, $\varrho_{N,Z}^{(\text{exc})}(\varepsilon)$ is multiplied with an exponential damping factor $\exp(-\varepsilon/T_0)$ as in Ref. [26]. For the parameter T_0 we use the critical temperature T_{crit} of the liquid-gas phase transition in symmetric nuclear matter of the DD2 parametrization. The maximum excitation energy in (108) is chosen as $E_{N,Z}^{(\max)} = 3(NS_{N,Z}^{(n)} + ZS_{N,Z}^{(p)})/5$ with the neutron and proton separation energies, $S_{N,Z}^{(n)}$ and $S_{N,Z}^{(p)}$, of the nucleus (N, Z) . For alternative approaches to treat the density of states for nuclei see Ref. [30].

References

1. W. Heisenberg, Z. Phys. **77**, (1932) 1-11.
2. E. Wigner, Phys. Rev. C **51**, (1937) 106-119.
3. C.F. von Weizsäcker, Z. Phys. **96**, (1935) 431-458.
4. H.A. Bethe and R.F. Bacher, Rev. Mod. Phys. **8**, (1936) 82-229.
5. B.K. Agrawal, J.N. De, S.K. Samaddar, G.Colò, and A. Sulaksono, Phys. Rev. C **87**, (2013) 051306.
6. J.M. Lattimer and Y. Lim, Ap. J. **771**, (2013) 51.
7. Bao-An Li and Xiao Han, arXiv:1304.3368 [nucl-th], Phys. Lett. B, in press.
8. H. Sotani, K. Nakazato, K. Iida, and K. Oyamatsu, Mon. Not. Roy. Astron. Soc. **434**, (2013) 2060.

9. Ning Wang, Li Ou, and Min Liu, *Phys. Rev. C* **87**, (2013) 034327.
10. K. Hebeler, J. M. Lattimer, C. J. Pethick, and A. Schwenk, *Ap. J.* **773**, (2013) 11.
11. Zhen Zhang and Lie-Wen Chen, *Phys. Lett. B* **726**, (2013) 234-238.
12. Jianmin Dong, Wei Zuo, and Jianzhong Gu, *Phys. Rev. C* **87**, (2013) 014303.
13. Lie-Wen Chen, arXiv:1212.0284 [nucl-th].
14. P. Marini et al., *Phys. Rev. C* **87**, (2013) 024603.
15. F.J. Fattoyev, J. Carvajal, W.G. Newton, and Bao-An Li, *Phys. Rev. C* **87**, (2013) 015806.
16. P. Russotto et al., *J. Phys.: Conf. Ser.* **420**, (2013) 012092.
17. F.J. Fattoyev, W.G. Newton, Jun Xu, Bao-An Li, *J. Phys.: Conf. Ser.* **420**, (2013) 012108.
18. Jianmin Dong, Wei Zuo, Jianzhong Gu, and Umberto Lombardo, *Phys. Rev C* **85**, (2012) 034308.
19. S. Gandolfi, *J. Phys.: Conf. Ser.* **420**, (2013) 012150.
20. W. Trautmann and H.H. Wolter, *Int. J. Mod. Phys. E* **21**, (2013) 1230003.
21. M.B. Tsang et al., *Phys. Rev. C* **86**, (2012) 015803.
22. K. Hagel et al., this volume.
23. S. Kowalski et al., *Phys. Rev. C* **75**, (2007) 014601.
24. J. Natowitz et al., *Phys. Rev. Lett.* **104**, (2010) 202501.
25. R. Wada et al., *Phys. Rev. C* **85**, (2012) 064618.
26. Ad.R. Raduta and F. Gulminelli, *Phys. Rev. C* **80**, (2009) 024606.
27. S. Typel, G. Röpke, T. Klähn, D. Blaschke, and H.H. Wolter, *Phys. Rev. C* **81**, (2010) 015803.
28. A.S. Botvina and I.N. Mishustin, *Nucl. Phys. A* **843**, (2010) 98-132.
29. M. Hempel and J. Schaffner-Bielich, *Nucl. Phys. A* **837**, (2010) 210-254.
30. M. Hempel, J. Schaffner-Bielich, S. Typel, and G. Röpke, *Phys. Rev. C* **84**, (2011) 055804.
31. M.D. Voskresenskaya and S. Typel, *Nucl. Phys. A* **887**, (2012) 42-76.
32. G. Röpke, N.-U. Bastian, D. Blaschke, T. Klähn, S. Typel, and H.H. Wolter, *Nucl. Phys. A* **897**, (2013) 70-92.
33. N. Buyukcizmeci et al., *Nucl. Phys. A* **907**, (2013) 1354.
34. H. Müller and B. D. Serot, *Phys. Rev. C* **52**, (1995) 2072-2091.
35. F. Gulminelli, Ad.R. Raduta, J. Margueron, P. Papakonstantinou, and M. Oertel, *J. Phys.: Conf. Ser.* **420**, (2013) 012079.
36. M. Hempel, V. Dexheimer, S. Schramm, and I. Iosilevskiy, *Phys. Rev. C* **88**, (2013) 014906.
37. Guang-Hua Zhang and Wei-Zhou Jiang, *Phys. Lett. B* **720**, (2013) 148-152.
38. P. Danielewicz and J. Lee, arXiv:1307.4130 [nucl-th].
39. D. Lunney, J.M. Pearson, and C. Thibault, *Rev. Mod. Phys.* **75**, (2003) 1021-1082.
40. P. Danielewicz, *Nucl. Phys. A* **727**, (2003) 233-268.
41. M. Wang, G. Audi, A.H. Wapstra, F.G. Kondev, M. MacCormick, X. Xu, and B. Pfeiffer, *Chinese Physics* **36**, (2012) 1603-2014.
42. J. Duflo and A.P. Zuker, *Phys. Rev. C* **52**, (1995) R23 and private communication to AMDC (<http://amdc.in2p3.fr>).
43. X. Viñas, M. Centelles, X. Roca-Maza, and M. Warda, arXiv:1308.1008 [nucl-th], this volume.
44. A. Carbone, A. Polls, C. Providência, A. Rios, and I. Vidaña, arXiv:1308.1416 [nucl-th], this volume.
45. M. Colonna, V. Baran, M. Di Toro, and H.H. Wolter, *Phys. Rev. C* **78**, (2008) 064618.
46. T. Klähn et al., *Phys. Rev. C* **74**, (2006) 035802.
47. C.J. Horowitz and A. Schwenk, *Phys. Lett. B* **638**, (2006) 153-159.
48. C.J. Horowitz and A. Schwenk, *Nucl. Phys. A* **776**, (2006) 55-79.
49. E. O'Connor, D. Gazit, C.J. Horowitz, A. Schwenk, and N. Barnea, *Phys. Rev. C* **77**, (2007) 055803.
50. G. Röpke, *Phys. Rev. C* **79**, (2009) 014002.
51. G. Röpke, *Nucl. Phys. A* **867**, (2011) 66-80.
52. C. Ducoin, Ph. Chomaz, and F. Gulminelli, *Nucl. Phys. A* **771**, (2006) 68-92.
53. G. Audi, F.G. Kondev, M. Wang, B. Pfeiffer, X. Sun, J. Blachot, and M. MacCormick, *Chinese Physics* **36**, (2012) 1157-1286.
54. M.K. Grossjean and H. Feldmeier, *Nucl. Phys. A* **444**, (1985) 113-132.
55. H.A. Bethe, *Phys. Rev.* **50**, (1936) 332-341.
56. H.A. Bethe, *Rev. Mod. Phys.* **9**, (1937) 69-249.